Astronomy & Astrophysics manuscript no. integral
April 23, 2008

Multi-wavelength observations of Galactic hard X-ray sources discovered by *INTEGRAL*. ⋆

I. The nature of the companion star

S. Chaty[1], F. Rahoui[2,1], C. Foellmi[3], J. A. Tomsick[4], J. Rodriguez[1], and R. Walter[5]

[1] Laboratoire AIM, CEA/DSM - CNRS - Université Paris Diderot, Irfu/Service d'Astrophysique, Bât. 709, CEA-Saclay, FR-91191 Gif-sur-Yvette Cedex, France, e-mail: chaty@cea.fr
[2] ESO, Alonso de Cordova 3107, Vitacura, Casilla 19001, Santiago 19, Chile
[3] Laboratoire d'Astrophysique, Observatoire de Grenoble, BP 53, F-38041 Grenoble Cedex 9, France
[4] Space Sciences Laboratory, 7 Gauss Way, University of California, Berkeley, CA 94720-7450, USA
[5] INTEGRAL Science Data Centre, Chemin d'Écogia 16, CH-1290 Versoix, Switzerland

Received April 23, 2008; accepted April 23, 2008

ABSTRACT

Context. (abridged) The *INTEGRAL* hard X-ray observatory has revealed an emerging population of highly obscured X-ray binary systems through multi-wavelength observations. Previous studies have shown that many of these sources are high-mass X-ray binaries hosting neutron stars orbiting around luminous and evolved companion stars.
Aims. To better understand this newly-discovered population, we have selected a sample of sources for which an accurate localisation is available to identify the stellar counterpart and reveal the nature of the companion star and of the binary system.
Methods. We performed an intensive study of a sample of thirteen *INTEGRAL* sources, through multi-wavelength optical to NIR photometric and spectroscopic observations, using EMMI and SofI instruments at the ESO NTT telescope. We performed accurate astrometry and identified candidate counterparts for which we give the optical and NIR magnitudes. We detected many spectral lines allowing us to determine the spectral type of the companion star. We fitted with stellar black bodies the mid-infrared to optical spectral energy distributions of these sources. From the spectral analysis and SED fitting we identified the nature of the companion stars and of the binary systems.
Results. Through spectroscopic analysis of the most likely candidates we found the spectral types of IGR J16320-4751, IGR J16358-4726, IGR J16479-4514, IGR J17252-3616, IGR J18027-2016: They all host OB type supergiant companion stars, with IGR J16358-4726 likely hosting an sgB[e]. Our spectra also confirm the supergiant O and B nature of IGR J17391-3021 and IGR J19140+0951. From SED fitting we found that IGR J16418-4532 is a (likely OB supergiant) HMXB, IGR J16393-4643 a (likely BIV-V star) HMXB, and IGR J18483-0311 a likely HMXB system. Through accurate astrometry, we rejected the proposed counterparts of IGR J17091-3624 and IGR J17597-2201, and we discovered two new candidate counterparts for each source, both suggesting an LMXB from SED fitting. We confirm the AGN nature of IGR J16558-5203. Finally, we report that NIR fields of four sources of our sample exhibit large-scale regions of absorption.
Conclusions.

Key words. Infrared: stars – X-rays: binaries, individuals: IGR J16320-4751, IGR J16358-4726, IGR J16393-4643, IGR J16418-4532, IGR J16479-4514, IGR J16558-5203, IGR J17091-3624, IGR J17252-3616, IGR J17391-3021, IGR J17597-2201, IGR J18027-2016, IGR J18483-0311, IGR J19140+0951 – Stars: supergiants

1. Introduction

The hard X-ray *INTEGRAL* observatory was launched on the 17th of October 2002, and since then, it has performed a detailed survey of the Galactic plane. The ISGRI detector on the IBIS imager (Lebrun et al. 2003) has discovered many new hard X-ray sources[1], including binary systems, pulsars and AGNs, all these so-called IGR sources being reported in Bird et al. (2007) and Bodaghee et al. (2007). One of the most important achievements of the *INTEGRAL* observatory to date is that it is revealing hard X-ray sources which were not easily detected in earlier soft X-ray (typically ≤ 10 keV) observations, bringing to light a previously hidden part of

Send offprint requests to: S. Chaty

⋆ Based on observations collected at the European Organisation for Astronomical Research in the Southern Hemisphere, Chile (ESO Programme 073.D-0339) (PI S. Chaty).

[1] An updated list of these sources is maintained at http://isdc.unige.ch/~rodrigue/html/igrsources.html.

a population of highly obscured high-energy binary systems in our Galaxy. These objects share characteristics that have rarely been seen (see Dean et al. 2005). They are high-mass X-ray binaries (HMXBs) hosting a neutron star orbiting an OB companion star, in some cases a supergiant star (see e.g. Filliatre & Chaty 2004 and Pellizza et al. 2006), some of them possibly being long-period X-ray pulsars. Many of these new sources are highly absorbed, exhibiting column densities higher than about 10^{23} cm^{-2}, and are concentrated in directions tangential to Galactic arms, for instance the Norma arm (see Chaty & Filliatre 2005, Tomsick et al. 2004a and Walter et al. 2004b), the richest arm of our Galaxy in high-mass star forming regions. This short-lived population hosts the likely progenitors of extremely compact binary objects, which are good candidates of gravitational wave emitters, and might constitute a key sample in the understanding of the evolution of high-energy binary systems.

Among these HMXBs hosting an OB supergiant companion star, two classes, which might overlap, appear (Chaty & Rahoui 2006). The first class is constituted of intrinsically highly obscured hard X-ray sources, exhibiting a huge local extinction. The most extreme example of these sources is the highly absorbed source IGR J16318-4848 (Filliatre & Chaty 2004). The second class exhibits fast and transient outbursts, with peak fluxes of the order of 10^{-9} erg s^{-1}cm^{-2} in the 20 – 40 keV band, and lasting only a few hours. This last characteristic is very unusual among HMXBs. For this reason they are called Supergiant Fast X-ray Transients (SFXTs, Negueruela et al., 2006b). These SFXTs have faint quiescent emission, and their hard X-ray spectra require a black hole or neutron star accretor. Among these sources, IGR J17544-2619 (Pellizza et al. 2006) seems to be the archetype of this new class of HMXBs, with long quiescent periods (Zurita Heras & Chaty in prep.).

Even if the *INTEGRAL* observatory can provide a localisation that is accurate above 10 keV ($\sim 2'$), it is not accurate enough to pinpoint the source at other wavelengths, which is necessary to reveal the nature of these sources. So the first step in the study of these sources is to look for an accurate localisation of the hard X-ray sources by X-ray satellites such as *XMM-Newton*, *Swift* or *Chandra*. While *XMM-Newton* and *Swift* provide positions good enough to restrict the list of possible counterparts to a small number, only *Chandra* gives unique identifications in most cases (see for instance the multi-wavelength study of four *INTEGRAL* sources in the direction of the Norma arm by Tomsick et al. 2006, via *Chandra* localisation). Once the source position is known to better than several arcseconds, the hunt for the optical counterpart of the source can begin. However, a difficulty persists, due to the high level of interstellar absorption in this region of the Galaxy, close to the Galactic plane. Near-infrared (NIR) observations, thanks to accurate astrometry, and photometric and spectroscopic analysis, allow for the nature of these sources to be revealed, constraining the spectral type of the companion star and the type of the binary system.

Finally, mid-infrared (MIR) observations are required to understand why these sources exhibit a strong local absorption, by characterizing the nature of the absorbing matter, and determining whether it is made of cold gas or dust, or anything else. Based on the optical/NIR observations we report here, we have performed MIR observations with the VISIR instrument on ESO VLT/UT3. These observations, focusing on the characterization of the presence, temperature, extension and composition of the absorbing material constituting the circumstellar medium enshrouding the obscured sources, are described in a companion paper by Rahoui et al. (2008).

Here we report on an intensive multi-wavelength study of a sample of 13 *INTEGRAL* sources belonging to both obscured and SFXT classes, for which accurate X-ray localisations are available, aimed at identifying their counterparts and constraining the nature of the companion star and of the binary system. We first describe the ESO optical/NIR photometric and spectroscopic observations, and build the spectral energy distributions (SEDs) in Section 2. We then review hard X-ray properties of each source, and report the results of our optical/NIR observations in Section 3. We give general results and discuss them in Section 4, and provide our conclusions in Section 5.

2. Observations

The multi-wavelength observations that we describe here are based on astrometry, photometry and spectroscopy on 13 *INTEGRAL* sources indicated in Table 1. They were performed at the European Southern Observatory (ESO, Chile), in 2 domains: in optical (0.4 – 0.8 μm) with the EMMI instrument and in NIR (1 – 2.5 μm) with the SofI instrument, both with the 3.5m New Technology Telescope (NTT) at La Silla Observatory. Our optical and NIR observations were carried out as part of the programme ESO # 073.D-0339, in the visitor mode[2].

2.1. Optical observations

On 2004 July 10 between UT 0.0 and 11.0 we obtained optical photometry in *B, V R, I* and *Z* bands of the sources given in Table 2 with the spectro-imager EMMI, installed on the NTT. We used the large field of EMMI's detector, with the images binned by a factor of 2, giving an image scale of $0\farcs332$/pixel and a field of view of $9\farcm0 \times 10\farcm0$. The photometric observations were performed with an integration time between 1 and 30 s for each exposure, as reported in Table 2. We observed five photometric standard stars of the optical standard star catalogue of Landolt (1992): PG 1633+099, PG 1633+099A; PG 1633+099B; PG 1633+099C and PG 1633+099D.

We also carried out optical spectroscopy on 2004 July 9, taking 30 spectra of the source IGR J17391-3021 with the low-resolution grism #1 of EMMI, with a slit of $1\farcs0$ providing a resolution of about 350, and a spectral range between 4370 and 10270 Å with a dispersion of about 7.3 Å. Each individual spectrum had an exposure time between 60 and 120 s, giving a total integration time between 720 and 1440 s, as reported in Table 3. We observed the spectro-photometric standard star LTT 7379 taken with a similar airmass to flux calibrate the optical spectra.

[2] The reduced data are available for retrieval at http://wikimbad.org.

Finally, through internal Director's Discretionary Time (DDT) we obtained long-slit low-resolution spectra of 2 sources –IGR J17252-3616 and IGR J18027-2016– with the spectro-imager EFOSC2 installed on the 3.6 m telescope of La Silla Observatory.

2.2. NIR observations

We performed NIR photometry in J, H and K_s bands of the sources given in Table 1 on 2004 July 08-11 with the spectro-imager SofI, installed on the NTT. We used the large field of SofI's detector, giving an image scale of 0.″288/pixel and a field of view of 4.′92×4.′92. The photometric observations were obtained by repeating a set of images for each filter with 9 different 30″ offset positions including the targets, following the standard jitter procedure allowing us to cleanly subtract the sky emission in NIR. The integration time varied between 10 and 50 s for each individual exposure, giving a total exposure time between 108 and 450 s. The NIR photometry results are given in Table 4. We observed three photometric standard stars of the faint NIR standard star catalogue of Persson et al. (1998): sj9157, sj9172 and sj9181.

We also carried out NIR spectroscopy with SofI between 0.9 and 2.5 μm, taking 12 spectra using alternatively the low-resolution Blue and Red grisms respectively, half of them with the 1.″0 slit on the source and the other half with an offset of 30″, in order to subtract the NIR sky emission. Each individual spectrum has an exposure time from 60 to 180 s, giving a total integration time between 720 and 2160 s in each grism, as reported in Table 3.

2.3. Data reduction

We used the IRAF (Image Reduction and Analysis Facility) suite to perform data reduction, carrying out standard procedures of optical and NIR image reduction, including flat-fielding and NIR sky subtraction.

We performed accurate astrometry on each entire SofI 4.′92 × 4.′92 field, using all stars from the 2MASS catalogue present in this field[3] (amounting to ∼ 1000 2MASS objects). The rms of astrometry fit is always less than 0.″5, and we obtained a pixel scale in x,y axis of −0.″28783 and 0.″28801/pixel respectively. The finding charts including the results of our astrometry are shown in Figures 2 and 3 for all sources of our sample.

We carried out aperture photometry, and we then transformed instrumental magnitudes into apparent magnitudes using the standard relation: $mag_{app} = mag_{inst} - Zp - ext \times AM$ where mag_{app} and mag_{inst} are the apparent and instrumental magnitudes, Zp is the zero-point, ext the extinction and AM the airmass. We used for the extinction $ext_{\rm J} = 0.06$, $ext_{\rm H} = 0.04$ and $ext_{\rm Ks} = 0.10$ typical of the La Silla observatory. The log of the observations and the results of photometry are given in Tables 2 and 4 for the optical and NIR respectively.

[3] The pixel size of 2MASS is 2.″0 and the position reconstruction error is ∼ 0.″2.

We analyzed the optical spectra using standard IRAF tasks, subtracting bias and correcting for flat field, and we used the *IRAF noao.twodspec* package in order to extract spectra and perform wavelength and flux calibrations. The optical spectra were reduced and flux-calibrated in "F-lambda" units - erg cm^{-2}s^{-1}Å.

NIR spectra were reduced using IRAF by flat-fielding, correcting the geometrical distortion using the arc frame, shifting the individual images using the jitter offsets, combining these images and finally extracting the spectra. The analysis of SofI spectroscopic data, and more precisely the sky subtraction, was difficult due to a variable sky, mainly in the red part of the blue grism, causing some wave patterns. The target spectra were then corrected for the telluric lines using a median of various standard stars observed with the same configuration during the corresponding nights. All spectra, optical and NIR, are finally shifted to the heliocentric rest frame.

2.4. SEDs

Once the most likely counterpart was identified through astrometry, photometry and spectroscopy when available, we were able to build the optical/NIR SEDs of all sources of our sample, shown in Figure 1. While these SEDs are mainly based on optical and NIR photometry from this paper, we also add MIR observations (5 − 20 μm) obtained with the VISIR instrument on Melipal, the 8 m third Unit Telescope (UT3) of the ESO Very Large Telescope (VLT) at Paranal Observatory, reported in the companion paper by Rahoui et al. (2008). We also put MIR data taken from the *Spitzer* GLIMPSE survey, reported in Rahoui et al. (2008), and in Table 5 for the sources not included in this companion paper. We include in these SEDs data from X-ray observations taken with *INTEGRAL*/IBIS for all the sources, *XMM* for IGR J16418-4532, IGR J17252-3616 and IGR J19140+0951, *RXTE* for IGR J16358-4726, IGR J17091-3624, IGR J17597-2201 and IGR J17391-3021, *ASCA* for IGR J16320-4751, IGR J16393-4643 and IGR J16479-4514, *BeppoSAX* for IGR J18027-2016, and finally *INTEGRAL*/JEM-X for IGR J18483-0311.

We fitted the optical to MIR observing data with a black body emission reproducing the stellar emission. The broad band SEDs of these sources were modelled using an absorbed black body emission component, representing the companion star emission (D_* and R_* are respectively the distance and radius of the star):

$$\lambda F(\lambda) = \frac{2\pi hc^2}{{D_*}^2 \lambda^4} 10^{-0.4 A_\lambda} \left[\frac{{R_*}^2}{e^{\frac{hc}{\lambda k T_*}} - 1} \right] \quad \text{in W.m}^{-2} \qquad (1)$$

The free parameters of the fits were the absorption in the V band $A_{\rm V}$, the companion star black body temperature T_* and its $\frac{R_*}{D_*}$ ratio. The fits were performed using a χ^2 minimization.

Best-fitting parameters for individual sources, as well as corresponding χ^2 and 90%–confidence ranges of parameters, are reported in Table 6 for the sources IGR J16393-4643, IGR J16418-4532, IGR J17091-3624, IGR J17597-2201, IGR J18027-2016 and IGR J18483-0311, and in Rahoui et al. (2008) for the remaining sources. The IGR J16558-5203 SED

has not been fitted, because of its AGN nature. In this Table we also give the interstellar extinction in magnitude, A_i, obtained from the neutral hydrogen column density $N_{\rm HI}$, and the X-ray extinction in magnitude, A_X, obtained from X-ray observations. Both extinctions were converted to magnitudes using the conversion between $N_{\rm H}$ and A_v given by Predehl & Schmitt (1995). $N_{\rm HI}$ has been computed using the $N_{\rm H}$ tool from HEASARC[4] (Dickey & Lockman 1990). Since $N_{\rm HI}$ is the total galactic column density along the line of sight, it is likely overestimated compared to the real value at the distance of the sources.

We overplot on the SEDs of Figure 1 the best-fitted model to our observations. The dip seen at $\sim 4\times10^{13}$ Hz is due to silicate absorption present in our extinction model (more details on this model are given in Rahoui et al. 2008).

3. Results on individual sources

All the sources studied in this paper were discovered with the IBIS/ISGRI detector onboard the *INTEGRAL* observatory. The sample of 13 sources, along with their position, uncertainty, and references about their discovery and position are given in Table 1. We present in the following our results on each source, for which we followed the same strategy. We first observed the field in optical and NIR, we performed accurate astrometry, and we derived the photometry of the candidates inside the X-ray satellite error circle. We then analyzed the optical/NIR spectrum of the most likely candidate, when available. We give the results of the optical-MIR SED fitting.

3.1. IGR J16320-4751

IGR J16320-4751 was discovered on 2003 February by Tomsick et al. (2003) at the position RA = $16^h32\overset{m}{.}0$, Decl. = $-47°51'$ (equinox J2000.0; uncertainty $2'$). Follow-up *XMM-Newton* observations localized the source at $16^h32^m01\overset{s}{.}9$ $-47°52'27''$ with $3''$ accuracy (Rodriguez et al. 2003; Rodriguez et al. 2006). It is a heavily absorbed variable source with $N_{\rm H} \sim 2.1\times10^{23}$ cm^{-2}, and a hard X-ray spectrum fitted by an absorbed power-law, with $\Gamma \sim 1.6$ (Rodriguez et al. 2006). Soft X-ray pulsations have been detected from this source at a period of P$\sim$ 1309$\pm$40 s with *XMM-Newton* and P$\sim$ 1295$\pm$50 s with *ASCA* observations, these pulsations being the signature of an X-ray pulsar (Lutovinov et al. 2005b). An orbital period of 8.96 $\pm$ 0.01 days was found from a *Swift*/BAT lightcurve extending from 2004 December 21 to 2005 September 17 (Corbet et al. 2005), and of 8.99$\pm$0.05 days with *INTEGRAL* (Walter et al. 2006). Putting the spin and orbital periods of this source on a Corbet diagram (Corbet 1986) suggests a supergiant HMXB nature. IGR J16320-4751 might have been persistent for at least 8 years, since this source is the rediscovery of a previously known *ASCA* source AX J1631.9-4752.

We performed accurate astrometry of the field (rms of fit=$0\overset{''}{.}49$), and overplot the $3''$ *XMM-Newton* error circle in the finding chart of Figure 2. We give the infrared magnitudes of all the candidate counterparts in Table 4. Two candidate counterparts had been proposed for this source (Rodriguez et al. 2003), however the *XMM-Newton* $3''$ error circle made the ambiguity disappear, accurately localizing the candidate labeled 1 in Figure 2, and making it the most likely counterpart (2MASS J16320215-4752289; Rodriguez et al. 2006). This result is in agreement with Negueruela & Schurch (2007) rejecting candidate 2 on the basis of 2MASS photometry. In addition, Candidate 1 is much more absorbed than Candidate 2, as can be seen from the optical and NIR magnitudes given for both candidate counterparts in Tables 2 and 4, since Candidate 1 is invisible in the optical, but becomes as bright as Candidate 2 in the K_S band. There are at least two faint candidate counterparts (labeled 3 and 4) inside the error circle, therefore it would be useful to obtain a more accurate position to unambiguously pinpoint the correct counterpart. However, the faintness of Candidates 3 and 4 tends to rule them out as counterparts, and in the following we will consider Candidate 1 as the most likely counterpart of this source.

NIR spectra of candidate 1 of IGR J16320-4751 are shown in Figure 4. We report the detected lines in Table 8. There are only a few lines visible in the blue NIR spectrum, probably because it is very faint and absorbed. The red NIR spectrum exhibits a very red continuum, and the presence of absorption and emission lines: the Pa(7-3) emission line, the Brackett series with P-Cygni profiles between 1.5 and 2.17 μm, and He I at 2.166 μm (perhaps with P-Cygni profile). The presence of these narrow and deep Paschen and He I lines, associated with P-Cygni profiles, are typical of early-type stars, and more precisely of luminous supergiant OB stars (Caron et al. 2003, Munari & Tomasella 1999), which is therefore the likely spectral type of the companion star. Furthermore, the presence of a wide Br γ emission line constrains the spectral type to a O supergiant or even O hypergiant (Hanson et al. 2005). We also took optical and NIR spectra of Candidate 2: they do not exhibit any emission lines, and seem typical of a late-type star. Such a spectral type would therefore be hard to reconcile with the wind accretion hard X-ray spectra and the localisation of this source in the Corbet diagram. Therefore both astrometry and spectroscopy allow us to exclude Candidate 2 as a candidate counterpart. These results strengthen Candidate 1 as the real counterpart of IGR J16320-4751. From the nature of the companion star and of the compact object, we derive that this source belongs to the very obscured supergiant HMXB class, hosting a neutron star. This result is also in agreement with the fit of its SED, computed in Rahoui et al. (2008) and shown in Figure 1.

3.2. IGR J16358-4726

IGR J16358-4726 was discovered on 2003 March 19 by Revnivtsev et al. (2003b) at the position (RA DEC J2000.0) = ($16^h35\overset{m}{.}8$, $-47°26'$, $1\overset{'}{.}5$ uncertainty). This hard X-ray source was observed for 25700 s serendipitously with *Chandra* during a scheduled observation of SGR 1627-41 on 2003 March 24. *Chandra* localized the source at ($16^h35^m53\overset{s}{.}8$, $-47°25'41\overset{''}{.}1$) with $0\overset{''}{.}6$ accuracy (Kouveliotou et al. 2003). We point out however that the uncertainty may be somewhat underesti-

[4] http://heasarc.gsfc.nasa.gov/cgi-bin/Tools/w3nh/w3nh.pl

Table 1. Sample of sources. Name and coordinates of the sources: position (RA, DEC, J2000.0), galactic longitude and latitude (l,b), uncertainty (Unc. in arcmin) and reference (Ref1) of the discovery of the source by *INTEGRAL*; and position (RA, DEC, J2000.0), uncertainty (Unc.) and reference (Ref2) of the most accurate position by the satellite indicated in parenthesis. References are b: Bodaghee et al. (2006), c: Chernyakova et al. (2003), h: Hannikainen et al. (2003), i: in't Zand et al. (2006), ke: Kennea & Capitanio (2007), ko: Kouveliotou et al. (2003), ku: Kuulkers et al. (2003), l3: Lutovinov et al. (2003), ma: Malizia et al. (2004), mo: Molkov et al. (2003), re2: Revnivtsev et al. (2003b), re4: Revnivtsev et al. (2004), ro: Rodriguez et al. (2006), sg: Sguera et al. (2007), sm: Smith et al. (2006), st: Stephen et al. (2005), su: Sunyaev et al. (2003), t3: Tomsick et al. (2003), t4: Tomsick et al. (2004b), w4: Walter et al. (2004a), w6: Walter et al. (2006), z: Zurita Heras et al. (2006).

Source	RA	DEC	l	b	Unc.	Ref1	RA	DEC	Unc.	Ref2
IGR J16320-4751	248.006	-47.875	336.3	0.169	0.4	t3	$16^h32^m01\overset{s}{.}9$	$-47°52'27''$	3″ (*XMM*)	ro
IGR J16358-4726	248.976	-47.425	337.01	-0.007	0.8	re2	$16^h35^m53\overset{s}{.}8$	$-47°25'41\overset{''}{.}1$	$0\overset{''}{.}6$ (*Chandra*)	ko
IGR J16393-4643	249.775	-46.706	338.015	0.100	0.7	ma	$16^h39^m05\overset{s}{.}4$	$-46°42'12''$	4″ (*XMM*)	b
IGR J16418-4532	250.468	-45.548	339.19	0.489	1.0	t4	$16^h41^m51\overset{s}{.}0$	$-45°32'25''$	4″ (*XMM*)	w6
IGR J16479-4514	252.015	-45.216	340.16	0.124	1.4	mo	$16^h48^m06\overset{s}{.}6$	$-45°12'08''$	4″ (*XMM*)	w6
IGR J16558-5203	254.010	-52.062	335.687	-05.493	2.0	w4	$16^h56^m05\overset{s}{.}73$	$-52°03'41\overset{''}{.}18$	$3\overset{''}{.}52$ (*Swift*)	st
IGR J17091-3624	257.280	-36.407	349.5	2.2	0.5	ku	$17^h09^m07\overset{s}{.}6$	$-36°24'24\overset{''}{.}9$	$3\overset{''}{.}6$ (*Swift*)	ke
IGR J17252-3616	261.299	-36.282	351.5	-0.354	0.5	w4	$17^h25^m11\overset{s}{.}4$	$-36°16'58\overset{''}{.}6$	4″ (*XMM*)	z
IGR J17391-3021	264.800	-30.349	358.07	0.445	1.2	su	$17^h39^m11\overset{s}{.}58$	$-30°20'37\overset{''}{.}6$	∼ 1″ (*Chandra*)	sm
IGR J17597-2201	269.935	-22.026	7.581	0.775	0.6	l3	$17^h59^m45\overset{s}{.}7$	$-22°01'39''$	4″ (*XMM*)	w6
IGR J18027-2016	270.661	-20.304	9.418	1.044	0.7	re4	$18^h02^m42\overset{s}{.}0$	$-20°17'18''$	4″ (*XMM*)	w6
IGR J18483-0311	282.068	-3.171	29.760	-0.744	0.8	c	$18^h48^m17\overset{s}{.}17$	$-03°10'15\overset{''}{.}54$	3.3″ (*Swift*)	sg
IGR J19140+0951	288.516	9.878	44.30	-0.469	0.5	h	$19^h14^m4\overset{s}{.}232$	$+09°52'58\overset{''}{.}29$	$0\overset{''}{.}6$ (*Chandra*)	i

Table 2. Results in Optical. We indicate the name of the source, the date and UT time of the observations, the airmass (AM), the exposure time in seconds (ET) and the B, V, R, I and Z magnitudes. Z-band magnitudes are instrumental.

Source	Date	AM	ET	B	V	R	I	Z
IGR J16320-4751 C1	2004-07-10T03:04	1.1	30	$> 22.79 \pm 0.27$	$> 24.70 \pm 0.46$	$> 22.10 \pm 0.26$	$> 22.31 \pm 0.25$	$> 21.67 \pm 0.42$
IGR J16320-4751 C2	2004-07-10T03:04	1.1	30	18.97 ± 0.04	16.62 ± 0.02	15.32 ± 0.01	13.23 ± 0.02	13.781 ± 0.003
IGR J16358-4726	2004-07-10T04:40	1.2	30	$> 23.42 \pm 0.28$	$> 23.67 \pm 0.33$	23.75 ± 0.34	20.49 ± 0.10	18.59 ± 0.08
IGR J16393-4643	2004-07-10T06:56	1.8	30	$> 24.97 \pm 0.80$	21.53 ± 0.13	19.62 ± 0.05	17.92 ± 0.05	16.99 ± 0.02
IGR J17391-3021	2004-07-10T06:22	1.3	1	$> 21.16 \pm 0.71$	14.97 ± 0.02	12.94 ± 0.02	11.28 ± 0.02	10.458 ± 0.001

Table 3. Log of optical and NIR spectra. We indicate the name of the source, the telescope used, the date and UT time of the observations, the airmass (AM), the exposure time in seconds in optical and NIR (blue and red grisms respectively). All spectra were obtained at ESO/NTT with EMMI and SofI instruments, except the optical spectra of IGR J17252-3616 and IGR J18027-2016 obtained at ESO/3.6m with EFOSC2.

Source	Tel	Date	AM	optical	NIR blue grism	NIR red grism
IGR J16320-4751 C1	NTT	2004-07-08T23:18	1.255	-	2160	2160
IGR J16320-4751 C2	NTT	2004-07-10T03:36	1.112	1440	-	-
”	NTT	2004-07-08T23:18	1.255	-	2160	2160
IGR J16358-4726	NTT	2004-07-09T02:06	1.052	-	2160	2160
IGR J16479-4514	NTT	2004-07-10T23:35	1.222	-	720	720
IGR J17252-3616	3.6m	2005-10-01T01:49	1.683	4800	-	-
”	NTT	2004-07-11T01:08	1.083	-	720	720
IGR J17391-3021	NTT	2004-07-10T05:36	1.177	720	-	-
IGR J17391-3021	NTT	2004-07-09T04:24	1.038	-	1080	1080
IGR J18027-2016	3.6m	2005-09-30T02:38	2.006	1800	-	-
”	NTT	2004-07-11T02:34	1.036	-	720	720
IGR J19140+0951	NTT	2004-07-11T04:38	1.289	-	720	720

mated since the source was $9\overset{'}{.}7$ from the *Chandra* aimpoint so that the point-spread function is significantly broadened. This source is a transient source, its hard X-ray spectrum being well fitted with a heavily absorbed power-law: $\Gamma \sim 0.5$ and $N_{\rm H} \sim 3.3\,10^{23}$ cm^{-2}, with the presence of Fe Kα emission line (Patel et al. 2007). By performing detailed spectral and timing analysis of this source using multi-satellite archival observations, Patel et al. (2007) have detected 5880 ± 50 s periodic variations, which could be due either to the spin of a neutron star, or to an orbital period, and they identified a 94 s spin-up in 8 days, corresponding to a mean spin period derivative of 1.9×10^{-4} s/s, pointing to a neutron star origin. Assuming that this spin up

Table 4. Results in NIR. We indicate the name of the source (C1, C2, etc. indicate the different candidates as labeled in the finding charts of Figure 2), the date and UT time of the observations, the airmass, the exposure time (Exptime) in seconds, and the J, H and K_S magnitudes.

Source	Date	Airmass	Exptime	J	H	K_S
			(s)	1.25 μm	1.65 μm	2.2 μm
IGR J16320-4751 C1	2004-07-08T23:05	1.3	108	17.24±0.11	13.28±0.04	11.21±0.05
IGR J16320-4751 C2	2004-07-08T23:05	1.3	108	12.30±0.03	11.41±0.03	11.05±0.05
IGR J16320-4751 C3	2004-07-08T23:05	1.3	108	18.86±0.20	17.70±0.17	16.85±0.15
IGR J16320-4751 C4	2004-07-08T23:05	1.3	108	-	-	18.21±0.33
IGR J16358-4726	2004-07-09T01:43	1.1	450	15.46±0.04	13.57±0.03	12.60±0.05
IGR J16393-4643 C1	2004-07-09T06:25	1.5	108	14.62±0.03	13.26±0.03	12.67±0.05
IGR J16393-4643 C2	2004-07-09T06:25	1.5	108	16.25±0.08	15.46±0.09	14.88±0.10
IGR J16393-4643 C3	2004-07-09T06:25	1.5	108	-	17.87±0.97	15.47±0.24
IGR J16393-4643 C4	2004-07-09T06:25	1.5	108	16.24±0.10	14.79±0.07	14.68±0.13
IGR J16418-4532 C1	2004-07-11T05:55	1.4	108	14.03±0.03	16.62±0.03	11.61±0.05
IGR J16418-4532 C2	2004-07-11T05:55	1.4	108	16.48±0.09	19.44±0.26	14.76±0.09
IGR J16418-4532 C3	2004-07-11T05:55	1.4	108	17.48±0.17	20.60±0.51	16.12±0.27
IGR J16418-4532 C4	2004-07-11T05:55	1.4	108	18.06±0.17	21.05±0.51	16.96±0.30
IGR J16479-4514 C1	2004-07-10T23:21	1.3	108	13.06±0.02	10.92±0.02	9.79±0.05
IGR J16479-4514 C2	2004-07-10T23:21	1.3	108	16.22±0.07	15.53±0.08	15.02±0.10
IGR J16558-5203	2004-07-11T06:18	1.5	108	12.82±0.03	11.66±0.03	10.52±0.05
IGR J17091-3624 C1	2004-07-11T06:35	1.5	108	16.73±0.05	15.83±0.05	15.36±0.07
IGR J17091-3624 C2	2004-07-11T06:35	1.5	108	18.19±0.11	17.12±0.12	16.65±0.14
IGR J17252-3616 C1	2004-07-11T00:39	1.2	108	14.19±0.02	11.90±0.03	10.67±0.05
IGR J17252-3616 C2	2004-07-11T00:39	1.2	108	17.40±0.10	15.13±0.05	13.92±0.07
IGR J17252-3616 C3	2004-07-11T00:39	1.2	108	-	15.00±0.06	13.82±0.09
IGR J17252-3616 C4	2004-07-11T00:39	1.2	108	-	18.61 1.17	15.17±0.13
IGR J17391-3021	2004-07-09T04:08	1.0	108	9.09±0.02	8.70±0.02	8.16±0.05
IGR J17597-2201 C1	2004-07-11T01:36	1.1	108	16.78±0.10	14.84±0.07	14.13±0.08
IGR J17597-2201 C2	2004-07-11T01:36	1.1	108	16.13±0.08	14.24±0.06	13.49±0.07
IGR J17597-2201 C3	2004-07-11T01:36	1.1	108	18.50±0.23	17.36±0.28	17.28±0.44
IGR J17597-2201 C4	2004-07-11T01:36	1.1	108	17.80±0.13	16.62±0.12	16.30±0.22
IGR J17597-2201 C5	2004-07-11T01:36	1.1	108	19.19±0.25	17.89±0.20	17.22±0.36
IGR J17597-2201 C6	2004-07-11T01:36	1.1	108	17.62±0.25	15.59±0.12	14.68±0.11
IGR J18027-2016 C1	2004-07-11T02:08	1.1	180	12.81±0.02	11.95±0.03	11.50±0.05
IGR J18027-2016 C2	2004-07-11T02:08	1.1	180	13.97±0.03	13.3±0.04	13.14±0.06
IGR J18027-2016 C3	2004-07-11T02:08	1.1	180	17.61±0.22	16.75±0.23	16.08±0.29
IGR J18027-2016 C4	2004-07-11T02:08	1.1	180	16.88±0.14	15.65±0.15	15.20±0.24
IGR J18483-0311	2004-07-11T07:44	1.7	180	10.77±0.03	9.21±0.03	8.39±0.04
IGR J19140+0951	2004-07-11T04:26	1.3	108	11.32±0.02	9.73±0.02	8.84±0.04

Table 5. GLIMPSE fluxes (in mJy) for the sources IGR J16393-4643, IGR J16418-4532, IGR J18027-2016 and IGR J18483-0535. The fluxes for the other sources are given in Rahoui et al. (2008).

Sources	3.6 μm	4.5 μm	5.8 μm	8 μm
IGR J16393-4643	3.53 ± 0.52	2.89 ± 0.47	–	–
IGR J16418-4532	12.46 ± 0.90	9.45 ± 0.58	5.57 ± 0.58	3.58 ± 0.41
IGR J18027-2016	10.70 ± 0.28	7.40 ± 0.18	5.30 ± 0.26	2.50 ± 0.05
IGR J18483-0535	217.00 ± 8.90	164.00 ± 7.20	124.00 ± 5.50	67.00 ± 2.10

is due to accretion, they estimate the source magnetic field to be between 10^{13} and 10^{15} G, suggesting that the compact object might be a magnetar. These observations suggest that this source is an X-ray pulsar at a distance of $\sim 6-8$ kpc. No radio emission has been detected.

A 2MASS counterpart has been suggested by Kouveliotou et al. (2003) based on the accurate *Chandra* position (2MASS J16355369-4725398, with J=15.41, H=13.44, K=12.59). We performed accurate astrometry of the field (rms of fit=0.″45), and overplot the 0.″6 *Chandra* error circle, as shown in Figure 2. The 2MASS counterpart is at 1.2″ from the centre, therefore outside the error circle. On the other hand, this 2MASS counterpart might be a blended object, since it shows an extension towards the east, right at the position of the error circle. A better spatial resolution would allow us to confirm or not whether the 2MASS candidate is the real

Table 6. Summary of parameters we used to fit the SEDs of the sources. We give their name, the interstellar extinction in magnitudes A_i, the X-ray extinction of the source in magnitudes A_X and the parameters of the fit: the extinction in the optical A_V, the temperature T_* and the $\frac{R_*}{D_*}$ ratio of the companion (more details on these parameters are given in the text). The 90%-confidence ranges of these parameters are given in parenthesis. We also give the reduced χ^2. The parameters for the other sources are given in Rahoui et al. (2008).

Sources	A_i	A_X	A_V	$T_*(K)$	$\frac{R_*}{D_*}$	χ^2/dof
IGR J16393-4643	11.71	133.61	11.5(10.9 – 11.8)	24400(12800 – 34200)	$2.21(1.81 - 3.13) \times 10^{-11}$	3.25/2
IGR J16418-4532	10.05	53.45	14.5(13.1 – 14.9)	32800(10600 – 36000)	$3.77(2.64 - 6.85) \times 10^{-11}$	1.5/4
IGR J17091-3624	4.13	5.34	6.8(2.0 – 9.6)	6900(3000, 34300)	$1.15(0.50 - 2.00) \times 10^{-11}$	1.005/1
IGR J17597-2201	6.251	24.05	16.1(13.1 – 17.1)	31700(6500 – 36000)	$1.28(1.30 - 3.00) \times 10^{-11}$	2.9/1
IGR J18027-2016	5.56	48.42	8.8(8 – 9.1)	20800(12800 – 32200)	$3.7(2.8 - 4.76) \times 10^{-11}$	6.00/4
IGR J18483-0535	8.66	148.1	17.4(16.9 – 18.3)	22500(16400 – 36000)	$2.15(1.75 - 2.75) \times 10^{-10}$	10/5

counterpart of this source. However, its brightness favors this candidate, and in the following we consider it as the candidate counterpart. Optical and NIR magnitudes of this 2MASS candidate are given in Tables 2 and 4 respectively.

The NIR spectra of IGR J16358-4726 are shown in Figure 4. We report the detected lines in Table 8. The NIR spectrum is very faint and extremely absorbed, however we detect some lines even in the blue part of its spectrum, mainly He II emission lines. The red part of the NIR spectrum exhibits a red continuum, and the presence of absorption and emission lines, with tentative P-Cygni profiles: the H Brackett series with P-Cygni profiles between 1.5 and 2.2 μm, and He I and He II absorption lines. The presence of these lines, associated with P-Cygni profiles, are typical of an OB supergiant star, which is therefore probably the spectral type of the companion star. In this case it would be a supergiant HMXB. In addtion, we clearly detect the forbidden [Fe II] line at 2.22 μm (and tentatively the allowed Fe II line at 1.98 μm), suggesting that the companion star is a sgB[e] star. Furthermore, it is interesting to note that Rahoui et al. (2008) propose, using an independent method of SED fitting, that the companion might be a sgB[e] star. Our result would therefore be in agreement with the fit of its SED, shown in Figure 1.

3.3. IGR J16393-4643

IGR J16393-4643 was discovered by Malizia et al. (2004) at the position (RA, DEC, J2000.0) = ($16^h39\overset{m}{.}3, -46°43'$) (2′ uncertainty). The improved position from *XMM-Newton*/EPIC is (RA DEC, J2000.0) = ($16^h39^m05\overset{s}{.}4, -46°42'12''$) (4″ uncertainty) which is compatible with that of 2MASS J16390535-4642137 (Bodaghee et al. 2006). It is a persistent, heavily-absorbed ($N_H = 2.5 \times 10^{23}$ cm^{-2}), and hard ($\Gamma = 1.3 \pm 1.0$) wind-accreting pulsar, and a pulse period of 912.0 ± 0.1 s was discovered in the ISGRI and EPIC light curves, characteristic of a spin period of an X-ray pulsar (Bodaghee et al. 2006). The high column density and hard spectral index suggest that IGR J16393-4643 is an HMXB. This source exhibits large variations in intensity, and shows X-ray lines. An orbital period of 3.6875 ± 0.0006 days has been detected in *Rossi-XTE* data, implying a mass function of $6.5 \pm 1.1\ M_\odot$ (or up to $14\ M_\odot$ if the orbit is eccentric; Thompson et al. 2006), this lower limit on the mass confirming that the system is an HMXB.

We performed accurate astrometry of the field (rms of fit=0.″54). Inside the error circle, there is the 2MASS candidate counterpart proposed by Bodaghee et al. (2006) (2MASS J16390535-4642137), and in addition there are 3 more candidates, labeled 1 to 4 in Figure 2. They are located at 1.7, 3.1, 3.4 and 3.″3 respectively from the centre of the error circle. Optical and NIR magnitudes of these candidates are given in Tables 2 and 4 respectively. A more precise localisation of the hard X-ray source is therefore necessary to know which is the real counterpart of the source, however Candidate 1 seems to be the most likely counterpart based on the astrometry and on its NIR brightness.

We fitted its SED with the model described in Section 2.4, taking the optical and NIR magnitudes of Candidate 1. We obtain a stellar temperature $T_* = 24400$ K, typical of a B spectral type companion star. The other parameters are given in Table 6, and the SED is shown in Figure 1. By taking the R_*/D_* ($= 2.21 \times 10^{-11}$) minimizing χ^2, and assuming a radius $R_* = 10\ R_\odot$ typical of a BIV-V spectral type companion star, we derive a distance of $D_* = 10.6$ kpc. On the other hand, by taking the minimum radius of a B supergiant star, i.e. at least $20\ R_\odot$, we derive a distance of nearly 20.4 kpc, probably too large to be plausible. The fit therefore is entirely consistent with its HMXB nature and favours a BIV-V companion star.

3.4. IGR J16418-4532

IGR J16418-4532 was discovered on 2003 February 1-5 at the position (RA DEC J2000.0) = ($16^h41\overset{m}{.}8$, $-45°32'$, 2′ uncertainty), towards the Norma region (Tomsick et al. 2004b). *XMM-Newton* localized the source at ($16^h41^m51\overset{s}{.}0, -45°32'25''$) with 4″ accuracy (Walter et al. 2006). *XMM-Newton* observations have shown that it is a heavily absorbed X-ray pulsar exhibiting a column density of $N_H \sim 1.0 \times 10^{23}$ cm^{-2}, a peak-flux of ~ 80 mCrab (20-30 keV), and a pulse period of 1246 ± 100 s (Walter et al. 2006). This source is an SFXT candidate, as proposed by Sguera et al. (2006) using *INTEGRAL* observations. A 3.75 day modulation was found in *Rossi-XTE*/ASM and *Swift*/BAT lightcurves, with

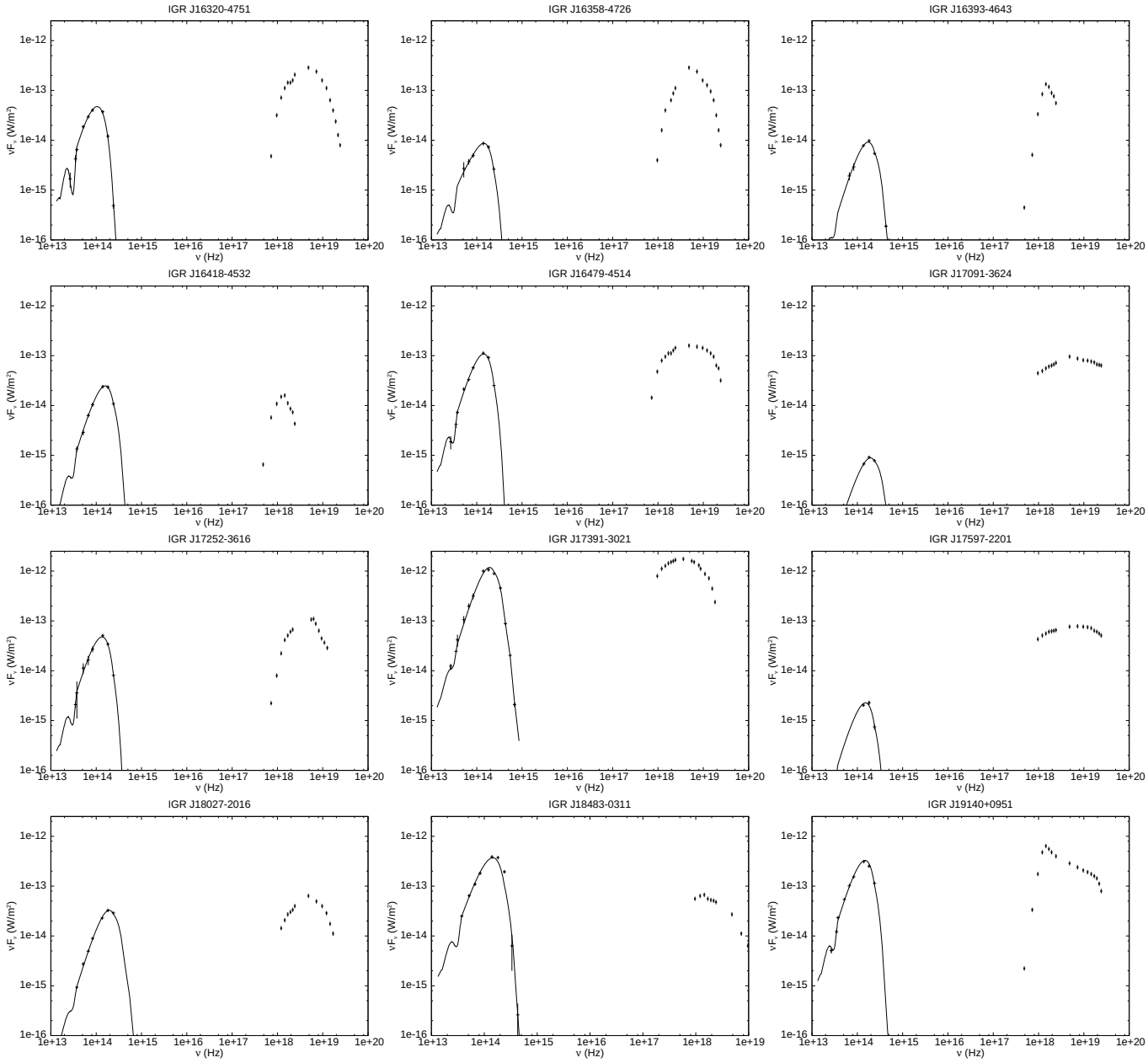

Fig. 1. SEDs of all these *INTEGRAL* sources, showing the observations from hard X-rays to MIR wavelengths. In each case, we overplot the black body emission representing the stellar spectral type of the companion star, which is given in Table 7 for the sources IGR J16393-4643, IGR J16418-4532, IGR J17091-3624, IGR J17597-2201, IGR J18027-2016 and IGR J18483-0535, and in Rahoui et al. (2008) for the remaining sources. See Section 2.4 for more details on the X-ray data. From top to bottom, and left to right: IGR J16320-4751, IGR J16358-4726, IGR J16393-4643, IGR J16418-4532, IGR J16479-4514, IGR J17091-3624, IGR J17252-3616, IGR J17391-3021, IGR J17597-2201, IGR J18027-2016, IGR J18483-0311 and IGR J19140+0951.

a possible total eclipse, which would suggest either a high binary inclination, or the presence of a supergiant companion star (Corbet et al. 2006). The latter case would be consistent with the position of this object in the Corbet diagram.

We performed the astrometry of this source with 1139 2MASS stars (rms of fit=0.″38). The field is shown in Figure 2. The centre of the *XMM-Newton* error circle is 2.″2 away from a bright 2MASS source (2MASS J16415078-4532253, labelled Candidate 1), as pointed out by Walter et al. (2006), however there are at least three more possible counterparts in the 4″ *XMM-Newton* error circle, not present in the 2MASS catalogue, at 1.9, 1.3 and 2.″1 respectively from the centre of the error circle. These additional candidate counterparts are labeled 2 to 4 respectively. We give their NIR magnitudes in Table 4. From the brightness in NIR we favor Candidate 1 as the candidate counterpart.

The fit of its SED, shown in Figure 1, and taking optical and NIR magnitudes as described in Section 2.4, gives a stellar temperature $T_* = 32800$ K, suggesting an OB spectral type companion star. The other parameters of the fit are given in

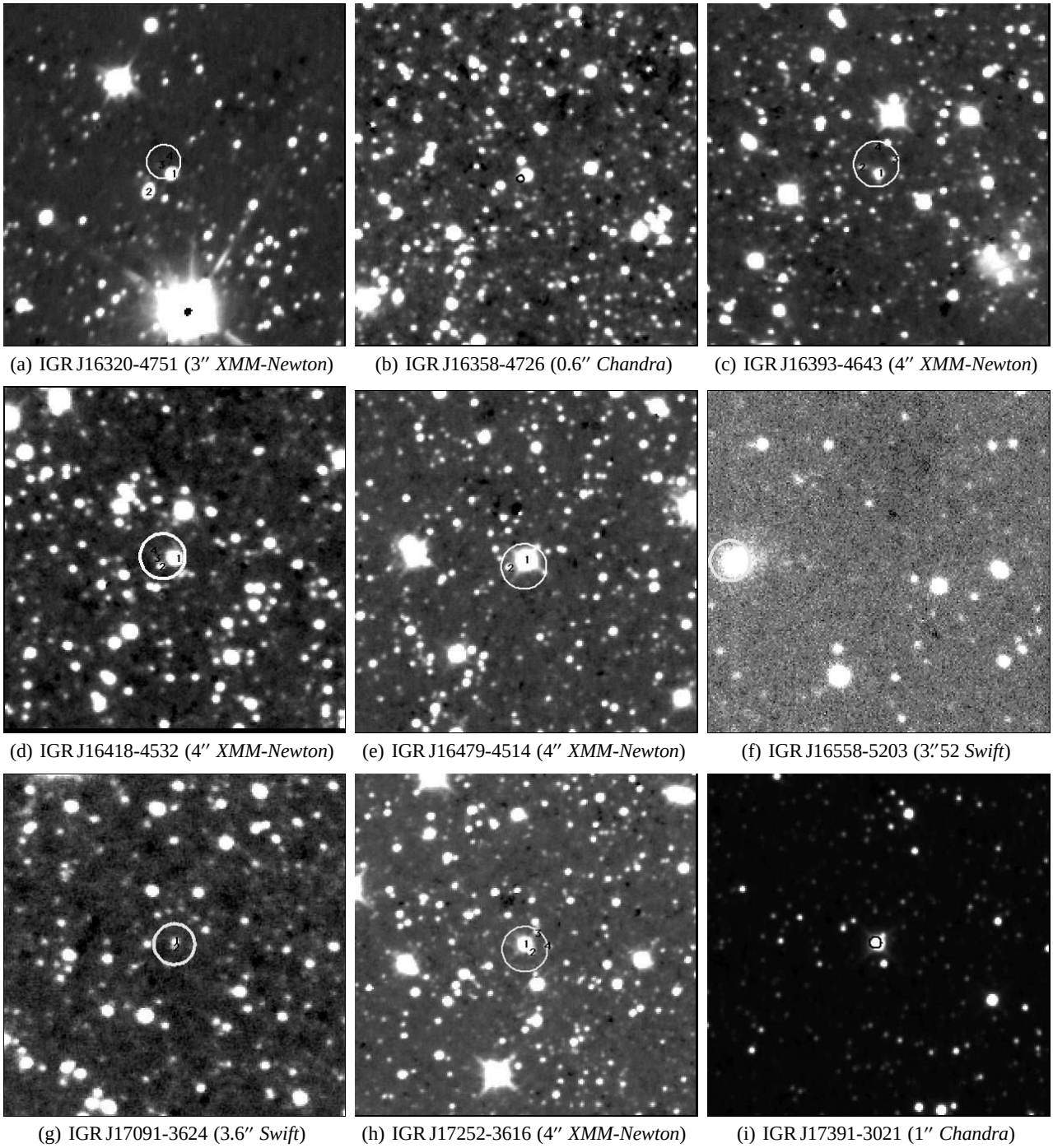

(a) IGR J16320-4751 (3″ *XMM-Newton*) (b) IGR J16358-4726 (0.6″ *Chandra*) (c) IGR J16393-4643 (4″ *XMM-Newton*)

(d) IGR J16418-4532 (4″ *XMM-Newton*) (e) IGR J16479-4514 (4″ *XMM-Newton*) (f) IGR J16558-5203 (3.″52 *Swift*)

(g) IGR J17091-3624 (3.6″ *Swift*) (h) IGR J17252-3616 (4″ *XMM-Newton*) (i) IGR J17391-3021 (1″ *Chandra*)

Fig. 2. Finding charts of the studied *INTEGRAL* sources, observed at ESO NTT telescope in the infrared K_S band (2.2 μm). Size: 1′x1′; North is to the top and East to the left. They are all centered apart from IGR J16558-5203, because the source was caught at the edge of the CCD. We overplot the most accurate localisation available to date.

Table 6. The R_*/D_* ratio which minimizes χ^2 ($= 3.77 \times 10^{-11}$) allows us to derive a minimal distance of 13 kpc for a supergiant, which is plausible. This source is therefore an HMXB, and could be a supergiant HMXB, consistent with its position in the Corbet diagram. We point out however its membership of the SFXT class is uncertain, based on its X-ray behaviour (Zurita Heras & Chaty in prep.).

3.5. IGR J16479-4514

IGR J16479-4514 was discovered on 2003 August 8-9 at the position (RA DEC J2000.0) = ($16^h47.^m9, -45°14'$), uncertainty $\sim 3'$, by Molkov et al. (2003). *XMM-Newton* observations localized the source at ($16^h48^m06.^s6, -45°12'08''$) with a 4″ accuracy (Walter et al. 2006). These *XMM-Newton* observations have shown a column density of $N_{\rm H} = 0.77 - 1.2 \times 10^{23}$ cm^{-2}. This source has recurrent outbursts, making it a fast transient

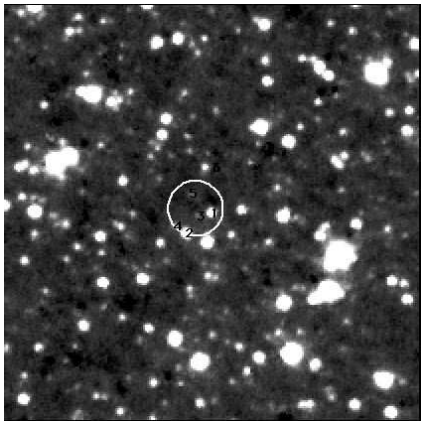

(a) IGR J17597-2201 (4″ *XMM-Newton*)

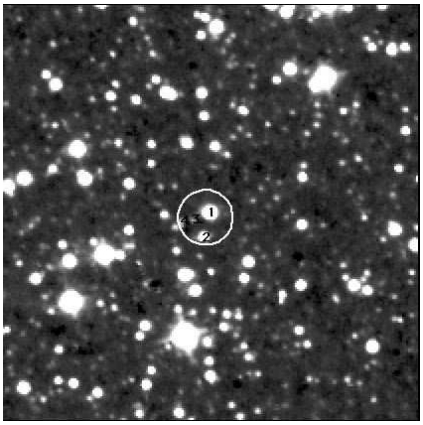

(b) IGR J18027-2016 (4″ *XMM-Newton*)

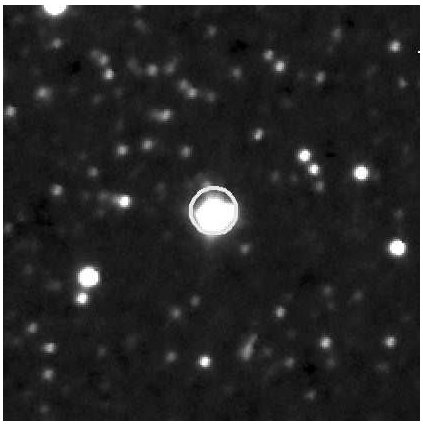

(c) IGR J18483-0311 (3.3″ *Swift*)

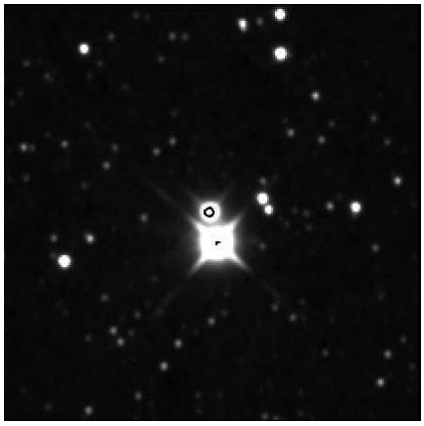

(d) IGR J19140+0951 (0.6″ *Chandra*)

Fig. 3. Figure 2 cont'd: finding chart of the studied *INTEGRAL* sources.

with a peak-flux of ∼ 120 mCrab (20-60 keV) (Sguera et al. 2005; Sguera et al. 2006). There is an IR source IRAS 16441-4506 in the error circle.

We performed accurate astrometry of the field (rms of fit= 0.″41), shown in Figure 2. There is a bright J = 12.9, H = 10.8 and K = 9.8 2MASS source (2MASS J16480656-4512068) 1.″1 away from the centre of the *XMM-Newton* error circle, which is the closest 2MASS source, suggested by Walter et al. (2006) as being a candidate counterpart. In addition, we find another candidate counterpart inside the error circle, at 2.″6 from the centre of the error circle, labeled 2 in Figure 2. The NIR magnitudes of both candidate counterparts are given in Table 4. However, on the basis of the astrometry (close to the error circle centre) and the photometry (NIR brightness) we favour Candidate 1 as the candidate counterpart.

NIR spectra of Candidate 1 are shown in Figure 4. We report the detected lines in Table 8. We find emission of H (Brackett series) between 1.5−2.17 μm, and also He I, He II and Fe II emission lines. These NIR spectra are typical of a supergiant OB star, therefore strengthening Candidate 1 as the likely counterpart of this source, the companion star of IGR J16479-4514 having an OB spectral type. Furthermore, the presence of a Br γ emission line and He I at 2.11 μm absorption line constrains the spectral type to a late O or peculiar early B supergiant (Hanson et al. 2005). This source would therefore be a supergiant HMXB system, probably belonging to the SFXT class. Its SED, consistent with the HMXB nature of the system, is shown in Figure 1.

3.6. IGR J16558-5203

IGR J16558-5203 was discovered at the position (RA DEC J2000.0) = ($16^h55.^m8, -52°03$) with a 2′ uncertainty (Walter et al. 2004a). This source has a *ROSAT* counterpart (1RXS J165605.6-520345) at the position ($16^h56^m05.^s60, -52°03'45.''5$), which allowed them to reduce the uncertainty to 8″ (Stephen et al. 2005). Recently, the position has been refined by *Swift* observations at ($16^h56^m05.^s73, -52°03'41.''18$) with a 3.″52 error circle radius (Malizia et al. 2007).

We performed accurate astrometry of the field, shown in Figure 2, and find that there is a bright 2MASS object inside the 3.″52 *Swift* error circle. The NIR magnitudes of this object are given in Table 4. This object is clearly extended on the NIR images, suggesting an extragalactic source. This is in agreement with the result from Masetti et al. (2006), who showed that this object is a Seyfert 1.2 AGN at a redshift of 0.054, exhibiting Hβ and O III emission lines.

3.7. IGR J17091-3624

IGR J17091-3624 was discovered at the position (RA DEC J2000.0) = ($17^h09\overset{m}{.}1, -36°24'38''$), uncertainty ~ 3′ (Kuulkers et al. 2003). Follow-up analysis of archival data from the TTM telescope aboard the KVANT module of the MIR orbital station revealed that this source had been detected in several observations performed on Oct.1-10, 1994, at the position (RA DEC J2000.0) = ($17^h09^m06^s, -36°24'07''$), error radius about 0.8′. This TTM position is within 0.6′ of the *INTEGRAL* position (Revnivtsev et al. 2003a). It is also coincident with the SAX source 1SAX J1709-36. A variable radio counterpart has been detected in follow-up radio observations at the position ($17^h09^m02\overset{s}{.}3 \pm 0.4, -36°23'33''$), giving an error circle of 5″ radius (Rupen et al. 2003). Since this source exhibited some radio emission it has been classified as a galactic X-ray binary, and a candidate microquasar, probably hosting a black hole. It exhibits a large variability in X-rays, and it is uncertain if this source is a Be/X-ray binary or an LMXB. Capitanio et al. (2006) confirm the low absorption ($N_{\rm H} \leq 1 \times 10^{22}$ cm^{-2}) and Comptonised spectrum of this source. Negueruela & Schurch (2007) proposed the 2MASS J17090199-3623260 source as a candidate counterpart, based on photometric catalogues. They report that this object is a late F8 V companion star. However, a more accurate position has been obtained by Kennea & Capitanio (2007): (RA DEC J2000.0) = ($17^h09^m07\overset{s}{.}6, -36°24'24\overset{''}{.}9$), error radius about 3.″6, which excludes the association of the high energy source with the radio source.

We have performed accurate astrometry of the field, shown in Figure 2, and we overplot the 3.″6 *Swift* error circle. We find that the claimed counterpart 2MASS J17090199-3623260 of Negueruela & Schurch (2007) is well outside this error circle; we can therefore reject it. We report the discovery of two blended candidate counterparts inside the error circle, labeled 1 and 2 in Figure 2 respectively, located at 0.″5 and 0.″4 from the centre of the error circle. We give the NIR magnitudes of these two candidate counterparts in Table 4. We need a more precise position in order to pinpoint the real counterpart of this source, but we favour Candidate 1 as the likely counterpart, on the basis of its NIR brightness.

With only three infrared magnitudes for the two candidate counterparts labeled C1 and C2, the fit of their SEDs is not very accurate, with the model described in Section 2.4. In addition, there is no counterpart of this source in the Spitzer GLIMPSE survey (3.6 and 4.5 μm). We can therefore not firmly conclude the nature of this binary system. However, it is interesting to note that the R_*/D_* 90% best fit values are very low ($= 1.15 \times 10^{-11}$). From these values we can compute the range of maximal radius that the massive star would have if it was at the maximal distance inside our Galaxy, at $D_* = 30$ kpc: we find $R_{*max} = [6.7 - 12.8]\ R_\odot$. Since the maximal radius of the companion star would be ~ 13 $R_\odot$, this star cannot be either a supergiant, or a giant. Alternatively, it could be a main sequence early-type star, but then located very far away in our Galaxy. We therefore conclude that this object is more probably an LMXB system in the Galactic bulge.

3.8. IGR J17252-3616

IGR J17252-3616 was discovered on 2004 February 9 in the Galactic bulge region, at the position ($17^h25\overset{m}{.}2, -36°16'$) by Walter et al. (2004a). Observations performed by *XMM-Newton* on 2004 March 21 by Zurita Heras et al. (2006) localized the source at ($17^h25^m11\overset{s}{.}4, -36°16'58\overset{''}{.}6$) with 4″ accuracy. This source is a rediscovery of the *EXOSAT* source EXO 1722-363, based on similar timing and spectral properties. It has been shown to be a heavily absorbed ($N_{\rm H} \sim 1.5 \times 10^{23}$ cm^{-2}) and persistent source, exhibiting apparent total eclipses, and a hard X-ray spectrum with either an absorbed Compton (kT~5.5 keV and $\tau \sim 7.8$) or a flat power law ($\Gamma \sim 0.02$), a very large column density, and Fe Kα line at 6.4 keV. The detection of a spin period of ~ 413.7 s and an orbital period of ~ 9.72 days securely classified this source as a binary X-ray Pulsar (Zurita Heras et al. 2006). Thompson et al. (2007) refined the orbital period to $P = 9.7403$ days with data collected over more than 7 years. They also derived a mass function of the system of 11.7 $M_\odot$, suggesting an HMXB nature. In addition, we point out that putting the spin and orbital periods of this source on a Corbet diagram (Corbet 1986) allows us to suggest a supergiant HMXB nature.

We performed accurate astrometry of the source, and overplot the *XMM-Newton* error circle, as shown in Figure 2. There is a bright 2MASS counterpart, 2MASS J17251139-3616575 (K_S=10.7, labelled Candidate 1), inside the error circle, as suggested by Walter et al. (2006). However, in addition to the 2MASS source, there are three fainter candidate counterparts inside the 4″ *XMM-Newton* error circle, labelled 2 to 4. All these candidates are located at 0.7, 1.4, 3.7 and 3.″9 from the centre of the error circle. One of these is blended with the 2MASS counterpart. IGR J17252-3616 would therefore benefit from a more accurate localisation, however based on astrometry and NIR brightness, we favour Candidate 1 as the most likely candidate counterpart. NIR magnitudes of these candidate counterparts are given in Table 4.

Optical and NIR spectra of the 2MASS counterpart (Candidate 1) are shown in Figure 5. We report the detected lines in Table 8. We find emission lines of H (Paschen and Brackett), He I and He II lines with likely P-Cygni profiles at 2.06 μm, and perhaps Fe II. From these NIR spectra, typical of an OB star, we conclude that the companion star of this source has an OB spectral type. Furthermore, the presence of He I in absorption and with P-Cygni profile constrains the spectral type to a B supergiant (Hanson et al. 2005). This result is in agreement with the suggestion by Zurita Heras et al. (2006), based on the presence of this bright 2MASS source in the error circle. This source is therefore an HMXB system, probably hosting a supergiant companion star, in agreement with the results by Thompson et al. (2007), and in agreement with its position in the Corbet diagram. The SED, consistent with the HMXB nature of the system, is shown in Figure 1.

3.9. IGR J17391-3021

IGR J17391-3021 was discovered on 2003 August 26 at the position (RA DEC J2000.0) = ($17^h39\overset{m}{.}1, -30°21\overset{'}{.}5$) with a

3′ uncertainty by Sunyaev et al. (2003). *Chandra* observations performed on 2003 October 15 localized the source at ($17^h39^m11\overset{s}{.}58, -30°20'37\overset{''}{.}6$) with ∼ 1″ accuracy (Smith et al. 2006). It is a rediscovery of a previously known *ASCA* and *Rossi-XTE* source AX J1739.1-3020 = XTE J1739-302 (Smith 2004). Negueruela et al. (2006a) have suggested that the optical counterpart of IGR J17391-3021 is a USNO A2.0 source (USNO B1.0 0596-058586) with B=17 and R=12.9, and that the NIR counterpart is a bright 2MASS source (2MASS J17391155-3020380 with J=8.600±0.021, H=7.823± 0.027 and K_S=7.428 ± 0.023; Smith et al. 2006). They also showed that the source is highly reddened, with a variable absorption column density between outbursts. During both low and high level states it exhibits hard X-ray spectra. The fast X-ray transient behaviour (typical of an SFXT) and neutron star spectrum have been confirmed by analyzing archival *INTEGRAL* data, with flares lasting between 30 min and 3 hours (Sguera et al. 2005), the bright ones reaching 330 mCrab (Türler et al. 2007). Negueruela et al. (2006a) state that this source is most likely an HMXB, however the outbursts are shorter than expected for HMXBs or Be/NS binaries, consistent with the SFXTs.

We performed accurate astrometry of the field (rms of fit=0.″47), and overplot the *Chandra* error circle, as shown in Figure 2. Optical and NIR magnitudes of the candidate counterpart are given in Tables 2 and 4 respectively. However the NIR magnitudes are out of the domain of linearity of SofI, which explains the discrepancy with the 2MASS magnitudes. We find that this 2MASS source is a blended source, however from the astrometry, it is clear that the 1″ *Chandra* error circle confirms that the 2MASS source is the counterpart of this source.

We examine the optical and NIR spectra shown in Figure 5. We report the detected lines in Table 8. In the optical spectrum, we first detect interstellar lines at 5800, 5890-6 (Na_I doublet), Hα, H lines (Paschen), He I and He II emission lines, N_I lines. The NIR spectrum is very rich in H lines from the Paschen and Brackett series, and also in He I and He II emission lines, some exhibiting P-Cygni profiles, and O I lines. All these lines are characteristic of early-type stars, more precisely of a supergiant O star, in agreement with the O8Iab(f) spectral type derived by Negueruela et al. (2006a). IGR J17391-3021 is therefore a supergiant HMXB, located at a distance of ∼ 2.3 kpc (Negueruela et al. 2006a), and not a Be as stated in Bird et al. (2006). The SED, consistent with the HMXB nature of the system, is shown in Figure 1.

We can determine the column density along the line of sight, using the equivalent width of the Na_I doublet=9 Å; E(B-V)=$0.25 \times W$(Å) = 2.25 magnitudes (using Munari & Zwitter (1997)); $N(\mathrm{H\,I} + H2) = 5.8 \times 10^{21} \times E(B-V) = 1.3 \times 10^{22}$ atoms/cm^2 (using Bohlin et al. 1978), the column density is consistent with the one indicated in Table 7.

3.10. IGR J17597-2201

IGR J17597-2201 was discovered at the position (RA DEC J2000.0) = ($17^h59\overset{m}{.}7, -22°01'$) with ∼ 2′ uncertainty (Lutovinov et al. 2003). *XMM-Newton* observations localized the source at ($17^h59^m45\overset{s}{.}7, -22°01'39''$) with a 4″ accuracy (Walter et al. 2006). It exhibits an absorption of $N_H = 4.5 \pm 0.7 \times 10^{22}$ cm^{-2}, or $2.70 \pm 0.15 \times 10^{22}$ cm^{-2} when a partial-covering absorber is included. This source, associated with the *Rossi-XTE* source XTE J1759-220, is a Low-Mass X-ray Binary system, a late-type transient type I X-ray burster, therefore hosting a neutron star, with a dipping behavior of ∼ 30% with ∼ 5 min dip duration (Markwardt & Swank 2003).

We performed accurate astrometry of the field, shown in Figure 2. Walter et al. (2006) proposed a 2MASS counterpart for this source (2MASS J17594556-2201435), however it is well outside the error circle, towards the south-west, at 5.″1 from the centre of the error circle. There are one bright and two faint candidate counterparts which are well inside the *XMM-Newton* error circle (labeled 1, 3 and 5 and located respectively at 2.25, 0.95 and 2.″05 from the centre of the *XMM-Newton* error circle). In addition, there are one faint and one bright candidate counterparts, lying on the error circle (labeled 2 and 4, and located respectively at 3.8 and 3.″9 from the centre of *XMM-Newton* error circle). We give the NIR magnitudes of these candidate counterparts in Table 4. Since the previously proposed counterpart is outside the error circle, and since we propose new candidate counterparts, this source deserves further observations to find which one is the right counterpart.

By fitting the SED of the brightest candidate labeled 1, which is also the closest to the error circle centre, with the model described in Section 2.4, we obtain a stellar temperature $T_* = 31700$ K, consistent with an O type star. The other parameters are given in Table 6, and the SED is shown in Figure 1. However our spectral fit is not accurate enough to unambiguously constrain the spectral type of the companion star, because we have only the three NIR magnitudes (we did not detect any MIR counterpart in the Spitzer GLIMPSE survey). Therefore, taking into account the errors, this SED fitting is consistent at 90% both with an LMXB and HMXB system. Assuming the source is a supergiant, with a minimum radius of 20 $R_\odot$, and taking a mean R_*/D_* of 2×10^{-11}, we obtain a distance of 35.2 kpc, which is not plausible. Alternatively, taking a radius $R_* = 10\ R_\odot$ typical of a B V companion star, we derive a distance of $D_* = 15.2$ kpc, a more reasonable estimate although still high. We therefore conclude that the source is most likely an LMXB, consistent with its X-ray properties, given the detection of type I X-ray bursts.

3.11. IGR J18027-2016

IGR J18027-2016 was discovered at the position (RA DEC J2000.0) = ($18^h02^m46^s, -20°16\overset{'}{.}3$) (Revnivtsev et al. 2004). *XMM-Newton* observations allowed to localize the source at ($18^h02^m42\overset{s}{.}0, -20°17'18''$) with 4″ accuracy (Walter et al. 2006). The source was originally called IGR J18029-2016, and it is associated with the SAX source SAX J18027-2017. The absorption is $N_H = 9.1 \pm 0.5 \times 10^{22}$ cm^{-2} (Walter et al. 2006). It is an X-ray pulsar, and a transient source, an eclipsing HMXB, likely at a distance of 10 kpc. An orbital period of 4.57 days and a pulse period of 139.47 s were reported by Hill et al. (2005). These authors have derived the system parameters, with an ex-

centricity of $e \leq 0.2$, a mass function of f(M)$\sim$ $17 \pm 5\ M_{\odot}$, implying a mass of the companion of $18.8 - 29.3\ M_{\odot}$.

We performed accurate astrometry of this source (rms of fit=0.″51), showed in Figure 2. There is a 2MASS counterpart (2MASS J18024194-2017172) at $\sim 1''$ from the centre of the *XMM-Newton* error circle, which is the candidate counterpart proposed by Walter et al. (2006). However there is another bright source well inside the error circle, labeled Candidate 2. There is also at least one faint counterpart inside the error circle. We give the NIR magnitudes of Candidate 1 and Candidate 2 in Table 4. Based on the proximity to the error circle centre, and its NIR brightness, we favour Candidate 1 as the likely candidate.

The optical and NIR spectra of Candidate 1 are shown in Figure 5. We report the detected lines in Table 8. In the optical spectrum we detect hydrogen (α to ζ) and He II emission lines, and in the NIR spectrum we detect H (Paschen and Brackett series), He I and He II emission lines, some tentatively exhibiting P-Cygni profiles. These NIR spectra are typical of a supergiant OB star, which is therefore likely the spectral type of the companion star: IGR J18027-2016 is therefore a supergiant HMXB system. Fitting the data with the model described in Section 2.4, we obtain a stellar temperature $T_* = 20800$ K, which is typical of a B supergiant star. The other parameters are given in Table 6, and the SED is shown in Figure 1. By taking the R_*/D_* minimizing χ^2 (3.7×10^{-11}), and assuming a typical radius of a B supergiant star, i.e. $R_* = 20\ R_{\odot}$, we derive a distance of $D_* = 11.9$ kpc. We therefore favour the supergiant nature of the companion star, with a B spectral type, in agreement with the results derived from the spectra.

3.12. IGR J18483-0311

IGR J18483-0311 was discovered at the position (RA DEC J2000.0) = ($18^h48^m3, -03°11'$), with uncertainty $\sim$ 2′ (Chernyakova et al. 2003). The *Swift* observations allowed Sguera et al. (2007) to refine the position of the source to ($18^h48^m17^s.17, -03°10'15.''54$), uncertainty 3.″3. The *Swift* refined position allowed them to identify an optical counterpart from the USNO-B1.0 and 2MASS catalogue located at ($18^h48^m17^s.2, -03°10'16.''5$) with magnitudes R=19.26, I=15.32, J=10.74, H=9.29 and K=8.46. The source exhibits a column density of $N_{\rm H} = 9{\times}10^{22}$ cm^{-2}, a $\Gamma = 1.4$ and an energy cutoff at $E_{cut} = 22$ keV (Sguera et al. 2007). Timing analysis of *Rossi-XTE*/ASM light curve have allowed investigators to derive an orbital period of 18.55 ± 0.05 days (Levine & Corbet 2006). Sguera et al. (2007) also report that the source contains a pulsar with a spin period of $21.0526{\pm}0.0005$ s with a pulse fraction of 65 ± 10%, while the highly reddened optical counterpart suggests by analogy with other such systems that the source is an HMXB. They further argue that it is a likely Be system due to its localisation in a Corbet diagram (Corbet 1986), but they cannot rule out an SFXT, although the typical ratio between maximum and minimum luminosity they observed is at least 10 times lower than that of typical SFXT.

We performed accurate astrometry of this source (rms of fit=0.″67), shown Figure 2. There is a bright 2MASS counterpart 2MASSJ 18481720-0310168 inside the *Swift* error circle, which is the candidate counterpart proposed by Sguera et al. (2007). However this source seems to be blended with another fainter source, at 2.5″ from the centre of the error circle. We give the NIR magnitudes of the bright candidate counterpart in Table 4.

Fitting the SED of this counterpart with the model described in Section 2.4 allows us to derive a stellar temperature of $T_* = 22500$ K at the limit of 90% of χ^2, which is typical of a B star. The other parameters are given in Table 6, and the SED is shown in Figure 1. The stellar temperature is consistent with a B spectral type companion star. Since the R_*/D_* ratio minimizing χ^2 is 2.15×10^{-10}, the distance of this source would then be 0.9 kpc if the companion star is a main sequence star (with a typical stellar radius of $R_* = 3\ R_{\odot}$), 1.5 kpc for a sub-giant and 2.7 kpc for a supergiant star (with a typical stellar radius of $R_* = 20\ R_{\odot}$). This source exhibits a strong NIR excess, which might indicate the presence of a disk/wind such as in massive stars. Furthermore, its position in the Corbet diagram is between Be and wind accretor-supergiant X-ray binary systems. Although we cannot firmly conclude on the spectral type and class, this SED shows that this source is an HMXB system.

3.13. IGR J19140+0951

IGR J19140+0951 was discovered on 2003 March 6-7 at the position (RA DEC J2000.0) = ($19^h13^m55^s, +9°51'.6$), uncertainty 1′) by Hannikainen et al. (2003). *Chandra* observations performed on 2004 May 11 localized the source at ($19^h14^m4^s.232, +09°52'58.''29$) with 0.″6 accuracy (in't Zand et al. 2006). Fitting the hard X-ray spectrum from *Rossi-XTE* observations allowed investigators to derive a $\Gamma \sim 1.6$ and $N_{\rm H} \sim 6 \times 10^{22}$ cm^{-2} (Swank & Markwardt 2003) with variations of $N_{\rm H}$ up to $\sim 10^{23}$ cm^{-2} (Rodriguez et al. 2005). An orbital period of 13.55 days was found from timing analysis of *Rossi-XTE* data, with an X-ray activity detected with *Rossi-XTE*/ASM as early as 1996 (Corbet et al. 2004), confirming the binary nature of the source. Rodriguez et al. (2005), after a comprehensive analysis of *INTEGRAL* and *Rossi-XTE* data, showed that the source was spending most of its time in a faint state but reported high variations of luminosity and absorption column density. It is a persistent HMXB with evidence for the compact object being a neutron star rather than a black hole, exhibiting a variable absorption column density, and a bright iron line (Rodriguez et al. 2005). This source has other names: IGR J19140+098 (Hannikainen et al. 2003), and EXO 1912+097. in't Zand et al. (2006) proposed the 2MASS source 2MASS J19140422+0952577 as the NIR counterpart of this source (J=8.55, H=7.67 and K_S= 7.06 magnitude).

We performed accurate astrometry of the field (rms of fit=0.″35), shown in Figure 2. The accurate error circle allows us to confirm the 2MASS source 2MASS 19140422+0952577 as the candidate counterpart, located at 4.″6 North of a bright 2MASS source (2MASS J19140417+0952538, K_S= 6.27 magnitude). We give the NIR magnitudes of the deblended candidate counterpart in Table 4. These deblended magni-

tudes we derive are different from the magnitudes given in the 2MASS catalogue, because both 2MASS sources are spatially very close in the 2MASS data.

We show the NIR spectra of this source in Figure 4. We report the detected lines in Table 8. The spectrum is dominated by H (Paschen and Brackett series), and He I and He II in emission. The NIR spectra are typical of an OB spectral type companion star, and the narrowness of the lines suggests a supergiant type, which is consistent with the results by Nespoli et al. (2007) for a B1I stellar type companion, derived from spectra obtained at ESO/NTT/SofI. This classification has been refined to B0.5I based on spectra obtained at UKIRT (Hannikainen et al. 2007), making IGR J19140+0951 a supergiant X-ray binary. Both classifications confirm the supergiant HMXB nature of IGR J19140+0951, hosting a neutron star. The SED, consistent with the HMXB nature of the system, is shown in Figure 1.

in't Zand et al. (2006) also suggest a MIR counterpart at 8.3 μm found in the Midcourse Space Experiment (*MSX*, Mill 1994), however Rahoui et al. (2008) show that in't Zand et al. (2006) are in fact reporting the summed flux of a blended source, composed of the MIR counterparts of both IGR J19140+0951 and the bright 2MASS source at the South, which is unrelated to IGR J19140+0951. Rahoui et al. (2008) give the MIR fluxes of the counterpart of IGR J19140+0951.

4. Discussion

We begin this Section by giving a summary of the results of all individual sources. We continue by showing the large scale environment of these sources, and report the presence of absorption in their environment. We then recall the general characteristics of HMXBs, before discussing the results obtained, in the context of the *INTEGRAL* era.

4.1. Summary of results of the sample of studied sources

We found by spectroscopy of the most likely candidate counterparts the spectral types of IGR J16320-4751, IGR J16358-4726, IGR J16479-4514, IGR J17252-3616 and IGR J18027-2016: they are all of supergiant OB types, IGR J16358-4726 likely hosting a sgB[e] companion star. We also confirm the supergiant O nature of IGR J17391-3021, and the supergiant B nature of IGR J19140+0951. By fitting the SED of the most likely candidates we found that IGR J16418-4532 is an HMXB, probably hosting a supergiant OB spectral type companion star, that IGR J16393-4643 is an HMXB system probably hosting a BIV-V companion star, and that IGR J18483-0311 is very likely an HMXB system. By accurate astrometry we rejected the counterpart proposed for IGR J17091-3624 and IGR J17597-2201, we propose two new candidate counterparts for each of them, which by SED fitting we found consistent with an LMXB nature. We confirm the AGN nature of IGR J16558-5203.

We summarize in Table 7 the results obtained both from spectroscopy and SED fitting to the sample of studied *INTEGRAL* sources. We give the results of the column density in optical/IR, spectral type of the companion stars, and type of sources for all individual sources of our sample. We also give all the parameters known about these sources, such as the spin and orbital period, and column density derived from X-ray observations, in order to facilitate the following discussion. The interstellar column density and absorption in the optical and NIR domain have been derived from our observations, given in Table 6 for the sources IGR J16393-4643, IGR J16418-4532, IGR J17091-3624, IGR J17597-2201, IGR J18027-2016 and IGR J18483-0535, and in Rahoui et al. (2008) for the remaining sources. We then converted the column density into absorption in magnitudes, using the relation given in Cardelli et al. (1989): $N_{\rm H}/A_{\rm v} = 1.87 \times 10^{21}$ cm^{-2}/ magnitudes.

The results, concerning the spectral type of the companion star, given by these SED fittings are in agreement with those directly derived from spectroscopy, when available. On the other hand, they allow us to derive the likely spectral type of the companion star, when there is no spectroscopic information. We can therefore conclude that most of these obscured sources host luminous, massive, hot and early-type companion stars, i.e. of OB spectral type, most of them being evolved stars of the supergiant spectral class.

From these SEDs, all reported in Figure 1, we can directly compare the optical to MIR with the hard X-ray domain integrated flux (corresponding to the energy output). All sources for which both fluxes are comparable are supergiant HMXBs: IGR J16418-4532, IGR J16479-4514, IGR J17252-3616, IGR J17391-3021, IGR J18027-2016, IGR J19140+0951. These comparable optical–MIR and hard X-ray fluxes are expected from the HMXB nature of the systems. Most of the sources for which the hard X-ray flux is much higher than the optical–MIR flux are HMXBs, hosting either a supergiant or B type companion star: IGR J16320-4751, IGR J16358-4726, IGR J16393-4643. IGR J17091-3624 and IGR J17597-2201 are the only cases with a hard X-ray flux higher than the optical–MIR flux, consistent with their LMXB nature. Finally, there is only one case where the hard X-ray flux is much less than the optical–MIR flux: the HMXB IGR J18483-0311. However we have to be cautious because the multi-wavelength observations of these SEDs were not taken simultaneously, and the hard X-ray fluxes are variable.

4.2. Environment

Four sources of the studied sample exhibit large-scale regions of absorption in the NIR images, very close to the line of sight of the hard X-ray source: IGR J16358-4726, IGR J16418-4532, IGR J16479-4514 and IGR J17391-3021. We show in Figure 6 the large field J band image of these sources (except for IGR J16479-4514 for which we show the large field K_S band image). This absorption region might be due to the presence of extended molecular clouds and/or H II regions. The presence of such highly absorbed regions is not surprising close to these peculiar hard X-ray sources, since they must be strongly linked to their formation. For instance, the Norma arm region is one of the richest star-forming regions of our Galaxy, where many high-mass stars form and evolve (Bronfman et al. 1996). There exists therefore a high probability for binary systems made up

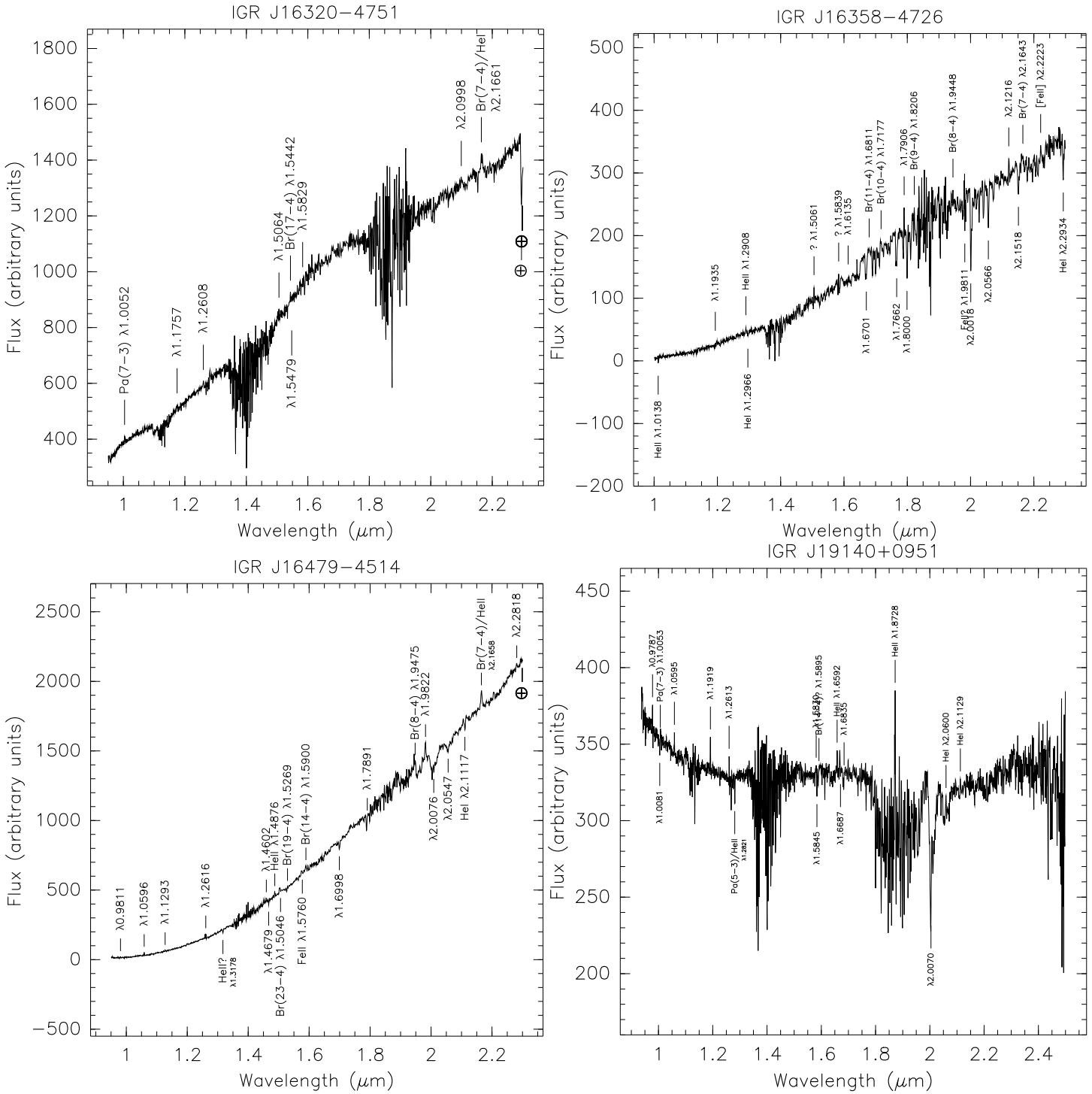

Fig. 4. From top to bottom, and left to right: combined blue and red grism NIR spectra of IGR J16320-4751 (Candidate 1), IGR J16358-4726, IGR J16479-4514 (Candidate 1) and IGR J19140+0951 (the y axis is in arbitrary units).

of high-mass stars to form, and evolve into HMXBs (see for instance Tauris & van den Heuvel 2006). This might explain why so many binary systems with high-mass companion stars and progenitors of compact objects such as black holes or neutron stars have formed in this region of our Galaxy.

Bodaghee et al. (2007) have compared the spatial distribution of HMXBs discovered by *INTEGRAL* –for which the distance is known– and of star-forming complexes, mainly OB regions reported by Russeil (2003). They have shown that their spatial distribution is similar, suggesting that HMXBs are associated with these complexes. The discovery of large-scale absorption regions in the direction of these sources is therefore not surprising, since the formation sites of HMXBs are closely linked to rich star forming regions. Indeed, the short life of HMXBs prevents these systems from migrating far away from their birthplace. Characterisation of these large-scale ab-

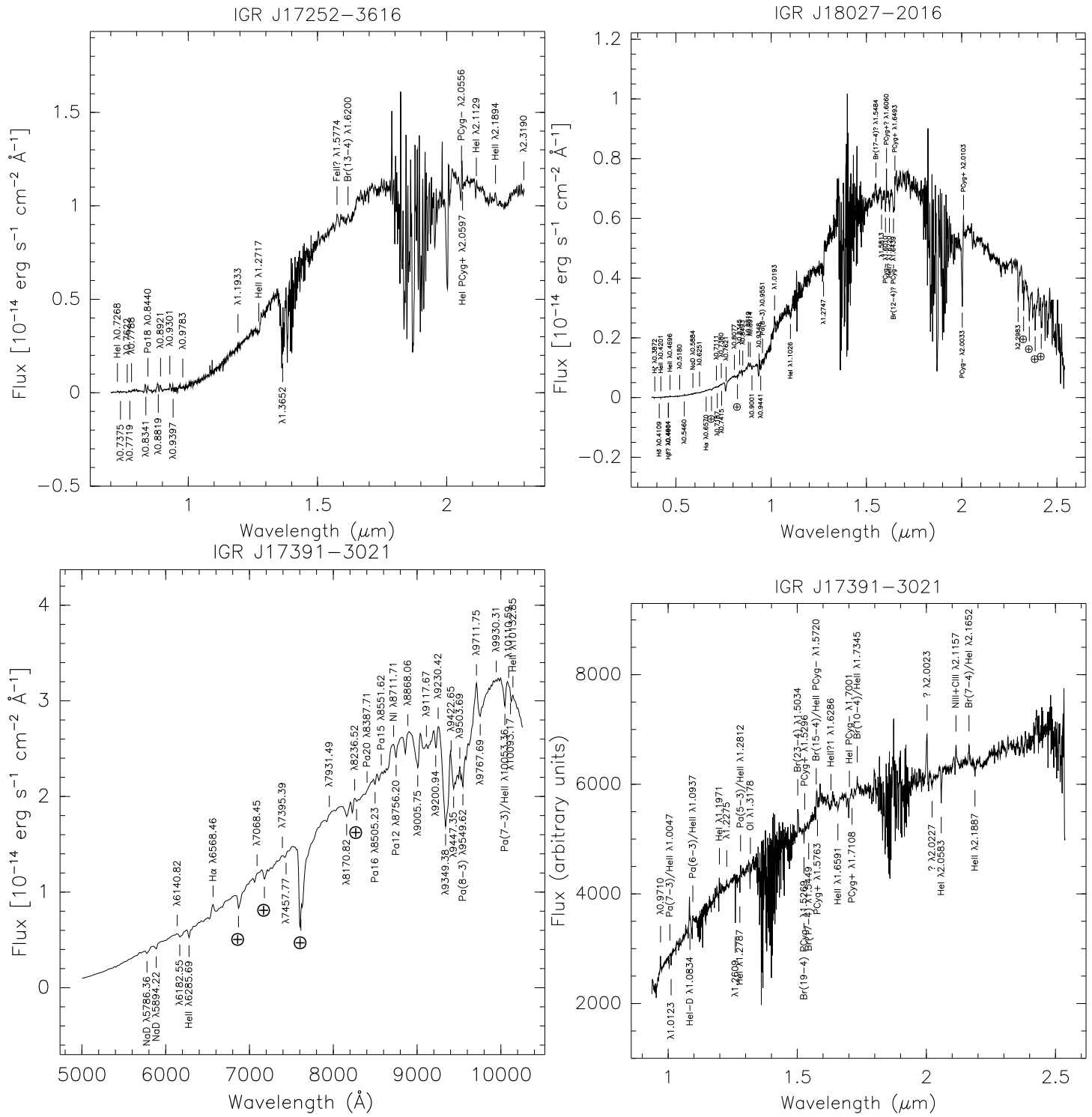

Fig. 5. Top panel: Combined flux calibrated spectra of the two sources IGR J17252-3616 Candidate 1 (left) and IGR J18027-2016 (right) respectively. The optical spectra were obtained with 3.6m/EFOSC, and the blue and red grism NIR spectra with NTT/SofI. We combined EFOSC2 and SofI spectra by applying a scaling factor of 18.4035 for IGR J17252-3616 and 2.417 for IGR J18027-2016, the difference being due to a different calibration between EFOSC2 and SofI, and to different exposure times. These two factors were obtained by dividing the flux in the overlap region between EFOSC2 and SofI spectra. The spectra are extremely red because of the galactic reddening. Besides the low S/N of the spectra, a number of narrow absorption lines could be detected. The y axis of the spectra are given in "λF_λ" units: erg s^{-1}cm^{-2}.
Bottom left panel: IGR J17391-3021 flux calibrated optical spectrum, with the y axis given in "λF_λ" units: erg s^{-1}cm^{-2}. Bottom right panel: combined blue and red grism NIR spectra of IGR J17391-3021, with the y axis in arbitrary units.

Table 7. Summary of results and characteristics of our studied sample of *INTEGRAL* sources. We give the name of the sources, the region of the Galaxy in the direction in which they are located, their spin and orbital period, the interstellar column density ($N_{\rm H}$I), the absorption derived from optical to infrared observations ($N_{\rm H}$IR), the absorption derived from X-ray observations ($N_{\rm H}$X), the spectral type (SpT) of their most likely candidate obtained or confirmed by spectroscopy (spec) or by fitting the SED (sed), the nature and type of the binary system, and the reference (Ref) to the spectral type. More details on each source are given in Section 3. Details on how we obtained $N_{\rm H}$I, $N_{\rm H}$IR and $N_{\rm H}$X are given in Section 2.4. Type abbreviations: AGN = Active Galactic Nucleus, B = Burster (neutron star), BHC = Black Hole Candidate, D = Dipping source, LMXB = Low-Mass X-ray Binary, HMXB = High-Mass X-ray Binary System, OBS = obscured source, SFXT = Supergiant Fast X-ray Transient, T: Transient source, XP: X-ray Pulsar. The classification as SFXT is still subjective, since we lack some accurate observations on a long-term scale for most of the sources. The spectral types come from optical/NIR spectroscopy, reported in the references given in the column Ref. c: this paper, h: Hannikainen et al. (2007), m: Masetti et al. (2006), neg: Negueruela et al. (2006a), nes: Nespoli et al. (2007).

Source	Region	Pspin (s)	Porb (d)	$N_{\rm H}$I 10^{22} cm^{-2}	$N_{\rm H}$IR 10^{22} cm^{-2}	$N_{\rm H}$X 10^{22} cm^{-2}	SpT	Nature	Ref
IGR J16320-4751	Norma	1250	8.96(1)	2.14	6.6	21	spec: sgO	HMXB/XP/T/OBS	c
IGR J16358-4726	Norma	5880		2.20	3.3	33	spec: sgB[e]?	HMXB/XP/T/OBS	c
IGR J16393-4643	Norma	912	3.6875(6)	2.19	2.19	24.98	sed: BIV-V?	HMXB/XP/T	c
IGR J16418-4532	Norma	1246	3.753(4)	1.88	2.7	10	sed: sgOB?	HMXB/XP/SFXT	c
IGR J16479-4514	Norma			2.14	3.4	7.7	spec: sgOB	HMXB/SFXT?	c
IGR J16558-5203	-	-	-	-	-	-	AGN	Seyfert 1.2	m
IGR J17091-3624	GC			0.77	1.03	1.0	sed: LMXB	BHC	c
IGR J17252-3616	GC	413	9.74(4)	1.56	3.8	15	spec: sgB	HMXB/XP/OBS	c
IGR J17391-3021	GC			1.37	1.7	29.98	spec: O8Iab(f)	HMXB/SFXT/OBS	neg
IGR J17597-2201	GC			1.17	2.84	4.50	sed: LMXB	LMXB/B/D/P	c
IGR J18027-2016	GC	139	4.5696(9)	1.04	1.53	9.05	spec: sgOB	HMXB/XP/T	c
IGR J18483-0311	GC	21.05	18.55	1.62	2.45	27.69	sed: HMXB?	HMXB/XP	c
IGR J19140+0951			13.558(4)	1.68	2.9	6	spec: B0.5I	HMXB/OBS	h, nes

sorption regions, and measurement of the metallicity of stars hosted by these regions are required to clarify this situation.

4.3. HMXBs in the INTEGRAL era

HMXBs are separated in two distinct groups. The first group contains the majority of the HMXB systems, constituted of known or suspected Be/X-ray Binary systems (BeXBs), called Be/X-ray transients. In Be systems, the donor is a Be star and the compact object is a neutron star typically in a wide, moderately eccentric orbit, spending little time in close proximity to the dense circumstellar disk surrounding the Be companion (Coe 2000; Negueruela 2004). X-ray outbursts occur when the compact object passes through the Be-star disk, accreting from the low-velocity and high-density wind around Be stars, and exhibiting hard X-ray spectra.

The second group of HMXB systems contains the Supergiant/X-ray Binaries (SXBs), where the compact object orbits deep inside the highly supersonic wind of a supergiant early-type star, which plays the role of the donor star (Kaper et al. 2004). The X-ray luminosity is powered either by accretion from the strong stellar wind of the optical companion, or by Roche-lobe overflow. In a wind-fed system, accretion from the stellar wind results in a persistent X-ray luminosity of 10^{35-36} erg/s, while in a Roche-lobe overflow system, matter flows via the inner Lagrangian point to form an accretion disc. In this case, a much higher X-ray luminosity ($\sim 10^{38}$ erg/s) is then produced during the outbursts.

In the pre-*INTEGRAL* era, known HMXBs were mostly BeXBs systems. For instance, in the catalogue of HMXBs of Liu et al. (2000), there were 54 BeXBs and 7 SXBs identified, out of 130 HMXBs, representing a proportion of 42% and 5% respectively. Then, between the two last editions of HMXB catalogues (Liu et al. 2000 and Liu et al. 2006), the proportion of SXBs compared to BeXBs has increased, with the first HMXBs identified in the *INTEGRAL* data. The third IBIS/ISGRI soft γ-ray survey catalogue (Bird et al. 2007), spanning nearly 3.5 years of operations, contains 421 sources detected with the *INTEGRAL* observatory, of which 214 ($\sim$ 50 %) were discovered by this satellite. This catalogue, extending up to 100 keV, includes 118 AGNs, 147 X-ray binaries (79 LMXBs and 68 HMXBs), 23 Cataclysmic Variables, 23 other objects, and 115 still unidentified objects. Among the 68 HMXBs, 24 have been identified as BeXBs and 19 as SXBs, representing a proportion of 35% and 28% respectively. The proportion of BeXBs, relative to the total of HMXBs, has decreased by a factor 1.2 while the proportion of SXBs has increased by a factor 5.6 between the catalogue of Liu et al. (2000) and the one of Bird et al.

(2007). Related to this increasing proportion of SXBs, the other highlight of the *INTEGRAL* catalogue is the emergence of the SFXT class, with 12 *INTEGRAL* sources being firm or possible candidates.

Our studied sample of *INTEGRAL* sources allows us to add four newly identified SXBs which were not classified as such in Bird et al. (2007): IGR J16320-4751, IGR J16358-4726, IGR J17252-3616 and IGR J18027-2016. The other sources that we have identified in this paper as supergiants were already considered SXBs, based either on spectral classification –IGR J17391-3021 and IGR J19140+0951– or on X-ray properties –the SFXT candidates IGR J16418-4532 and IGR J16479-4514–. With these new SXBs, the proportion of SXBs has reached that of BeXBs: 35% of all HMXBs for each population. This clearly shows that the launch of *INTEGRAL* has drastically changed the statistical situation concerning the nature of HMXBs, by revealing a new dominant population of supergiant X-ray binaries, which are purely wind accretor systems.

Although this came as a surprise, it is *a posteriori* consistent with the fact that these hard X-ray emitters are sources ideally detected by *INTEGRAL*, as discussed in Lutovinov et al. (2005a), Dean et al. (2005) and Bodaghee et al. (2007). *INTEGRAL*, observing at energies higher than the threshold above which photoelectric absorption becomes negligible in most matter, can easily detect bright sources above a few tens of keV, while they are not detectable below, and therefore had remained hidden up to now. HMXBs accreting by stellar wind create a naturally dense and highly absorbing circumstellar wind compared to Roche lobe overflow in LMXBs, hiding the X-ray emission in a similar way to Seyfert 2 AGNs (Dean et al. 2005; Malizia et al. 2003).

4.4. The nature of *INTEGRAL* HMXBs

Let us now consider our results, summarized and put together with other characteristics of these sources in Table 7. In this sample of 13 *INTEGRAL* sources, concentrated both towards the direction of the Norma arm and the Galactic centre, we classified 10 HMXBs (8 sources hosting sgOB and 2 sources hosting BIV-V companion stars), 2 LMXBs and 1 AGN. We clearly confirm the predominance of HMXBs hosting supergiants, as opposed to those hosting Be companion stars: in our sample, 80% of HMXBs host compact objects (probably neutron stars) orbiting around OB supergiant secondaries. As already discussed, this result is in agreement with the increase of SXBs in the HMXBs population. However, quantitatively, the proportion of SXBs in our studied sample is higher than in the Bird et al. (2007) catalogue. There are two reasons: first, our sample is much more limited; second, most of the sources of our sample are in the direction of the Norma arm, which is associated with rich star-forming regions, the natural birthplace of massive stars, as discussed in Section 4.2. Most of these new *INTEGRAL* sources are wind accretors, consistent with their location in the Corbet diagram (Corbet 1986): nearly all of the HMXBs discovered by *INTEGRAL*, for which both spin and orbital periods have been measured, are located in the upper part of this diagram, among other wind accretors, typical of supergiant HMXBs. These systems exhibit extra absorption by a factor of ~ 4 compared to the average of all HMXBs, and they are X-ray pulsars, with longer pulsation periods than previously known HMXBs (Bodaghee et al. 2007).

In the companion paper by Rahoui et al. (2008) it is shown that only 3 sources –IGR J16318-4848, IGR J16358-4726 and IGR J16195-4945– of a sample of 12 *INTEGRAL* sources exhibit a MIR excess, due to an absorbing component enshrouding the whole binary system. The MIR emission of the remaining sources comes from the supergiant companion star, showing that absorbing material is enshrouding the compact object for most of the sources (preliminary results of this paper were described in Chaty & Rahoui 2006). We are therefore observing two classes of *INTEGRAL* sources, i.e. highly absorbed sources such as IGR J16358-4726, for which the extreme representant is IGR J16318-4848, and SFXTs such as IGR J17391-3021, for which the archetype is IGR J17544-2619.

As shown in Table 7, these classes share similar properties –for instance they both host supergiant companion stars– however they do not seem to have exactly the same configuration, and one way to explain their different characteristics can be found in their excess in absorption, which does not seem to have the same origin. It is caused by two different phenomena in the case of the highly absorbed sources: the observations from hard X-ray to MIR domains suggest the presence of absorbing material concentrated around the compact object, and also some dust and/or cold gas, perhaps forming a cocoon, enshrouding the whole binary system (Filliatre & Chaty 2004; Rahoui et al. 2008). Their characteristics might be explained by the presence of a compact object (neutron star or black hole) orbiting within the dense wind surrounding the companion star. On the other hand, in the case of SFXTs, characterised by fast X-ray outbursts, the presence of the absorbing material seems concentrated around the compact object only, and MIR observations show that there is no need for any other absorbing material around the whole system (Rahoui et al. 2008). Their characteristics might be explained by the presence of a compact object (neutron star or black hole) located on an eccentric orbit around the companion star, and it would then be when the compact object penetrates the clumpy circumstellar envelope that outbursts are caused. However the situation is more complicated, since some SFXT sources are also highly obscured, and the intrinsic absorption derived from X-ray observations vary for some *INTEGRAL* sources (see e.g. the case of IGR J19140+0951; Prat et al. 2008).

The X-ray transient or persistent nature of these sources might therefore be related to the geometry of these systems, and it is possible to distinguish the nature of both classes by speculating on the geometry of these systems (see also Chaty & Rahoui 2006). However only the knowledge of their orbital periods, which is currently unknown for most of these sources, will allow us to confirm or not this view. Many questions are still open, most of them related to the interaction between the compact object and the supergiant star, and to the nature of the absorbing material, which seems to be present in the environment either of the compact object, or of the whole binary system, and even both. To better understand the gen-

eral properties of these systems, we will need to better characterise the dust, its temperature, composition, geometry, extension around the system, and to investigate where this dust or cold gas comes from. Finally, probably the most important question to solve is whether this unusual circumstellar environment is due to stellar evolution OR to the binary system itself. To answer this question, this dominant population of supergiant HMXBs now needs to be taken into account in population synthesis models.

5. Conclusions

We have performed an extensive study of a sample of 13 *INTEGRAL* sources, through optical and NIR photometry and spectroscopy, performing for each source accurate astrometry, identifying candidate counterparts, deriving their optical and NIR magnitudes, and obtaining spectra for most of them. In addition, we built and fitted the SED of these sources, from MIR to hard X-rays. We thus identified the nature of the companion stars and of the binary systems by spectroscopy for 7 of these sources, and by fitting their SED for 5 of them. We finally reported NIR fields of four of these sources, which exhibit large-scale regions of absorption, probably linked to their formation process. We then discussed the existence of this dominant population of supergiant HMXBs in our Galaxy, born with two very massive components: a population which only recently has been revealed by the *INTEGRAL* observatory.

Thus, it clearly appears that a study of this new population of supergiant HMXBs, constraining the nature and orbital parameters of these systems, and linking them to population synthesis models, will provide a better understanding of the evolution of HMXBs. These systems are probably the primary progenitors of neutron star/neutron star or neutron star/black hole mergers. There is therefore the possibility that they are related to short/hard γ-ray bursts, and also that they might be good candidates for gravitational wave emitters. Because most of these sources are obscured, the "Norma arm"-like sources can only be studied in the hard X-ray and infrared domains. A joint study of these sources with multi-wavelength hard X-ray, optical, NIR, MIR (and radio) observations is therefore necessary.

Acknowledgements. Based on observations collected at the European Organisation for Astronomical Research in the Southern Hemisphere, Chile (ESO Programme 073.D-0339). We acknowledge Jorge Melnick for special DDT time at 3.6 telescope on EFOSC2. SC thanks the ESO staff and especially Valenti Ivanov and Emanuela Pompei for their invaluable assistance during the run when we performed these optical and NIR observations. JAT acknowledges partial support from *Chandra* award number GO5-6037X issued by the *Chandra X-Ray Observatory Center*, which is operated by the Smithsonian Astrophysical Observatory for and on behalf of the National Aeronautics and Space Administration (NASA), under contract NAS8-03060. This research has made use of NASA's Astrophysics Data System, of the SIMBAD database, operated at CDS, Strasbourg, France, and of data products from the Two Micron All Sky Survey, which is a joint project of the University of Massachusetts and the Infrared Processing and Analysis Center/California Institute of Technology, funded by the National Aeronautics and Space Administration and the National Science Foundation.

References

Bird, A. J., Barlow, E. J., Bassani, L., et al. 2006, ApJ, 636, 765
Bird, A. J., Malizia, A., Bazzano, A., et al. 2007, ApJS, 170, 175
Bodaghee, A., Courvoisier, T. J.-L., Rodriguez, J., et al. 2007, A&A, 467, 585
Bodaghee, A., Walter, R., Zurita Heras, J. A., et al. 2006, A&A, 447, 1027
Bohlin, R. C., Savage, B. D., & Drake, J. F. 1978, ApJ, 224, 132
Bronfman, L., Nyman, L.-A., & May, J. 1996, A&AS, 115, 81
Capitanio, F., Bazzano, A., Ubertini, P., et al. 2006, ApJ, 643, 376
Cardelli, J. A., Clayton, G. C., & Mathis, J. S. 1989, ApJ, 345, 245
Caron, G., Moffat, A. F. J., St-Louis, N., Wade, G. A., & Lester, J. B. 2003, AJ, 126, 1415
Chaty, S. & Filliatre, P. 2005, Ap&SS, 297, 235
Chaty, S. & Rahoui, F. 2006, in The Obscured Universe, Procs. of 6th INTEGRAL workshop, Moscow, Russia, July 2-8, 2006, to be published by ESA's Publications Division in December 2006 as Special Publication SP-622, in press (astro-ph/0609474)
Chernyakova, M., Lutovinov, A., Capitanio, F., Lund, N., & Gehrels, N. 2003, The Astronomer's Telegram, 157, 1
Coe, M. J. 2000, in ASP Conf. Ser. 214: IAU Colloq. 175: The Be Phenomenon in Early-Type Stars, ed. M. A. Smith, H. F. Henrichs, & J. Fabregat, 656–+
Corbet, R., Barbier, L., Barthelmy, S., et al. 2006, The Astronomer's Telegram, 779, 1
Corbet, R., Barbier, L., Barthelmy, S., et al. 2005, The Astronomer's Telegram, 649, 1
Corbet, R. H. D. 1986, MNRAS, 220, 1047
Corbet, R. H. D., Hannikainen, D. C., & Remillard, R. 2004, The Astronomer's Telegram, 269, 1
Dean, A. J., Bazzano, A., Hill, A. B., et al. 2005, A&A, 443, 485
Dickey, J. M. & Lockman, F. J. 1990, ARA&A, 28, 215
Filliatre, P. & Chaty, S. 2004, ApJ, 616, 469
Hannikainen, D. C., Rawlings, M. G., Muhli, P., et al. 2007, MNRAS, 380, 665
Hannikainen, D. C., Rodriguez, J., & Pottschmidt, K. 2003, IAU Circ., 8088, 4
Hanson, M. M., Kudritzki, R.-P., Kenworthy, M. A., Puls, J., & Tokunaga, A. T. 2005, ApJS, 161, 154
Hill, A. B., Walter, R., Knigge, C., et al. 2005, A&A, 439, 255
in't Zand, J. J. M., Jonker, P. G., Nelemans, G., Steeghs, D., & O'Brien, K. 2006, A&A, 448, 1101
Kaper, L., van der Meer, A., & Tijani, A. H. 2004, in Revista Mexicana de Astronomia y Astrofisica Conference Series, ed. C. Allen & C. Scarfe, 128–131
Kennea, J. A. & Capitanio, F. 2007, The Astronomer's Telegram, 1140, 1
Kouveliotou, C., Patel, S., Tennant, A., et al. 2003, IAU Circ., 8109, 2
Kuulkers, E., Lutovinov, A., Parmar, A., et al. 2003, The

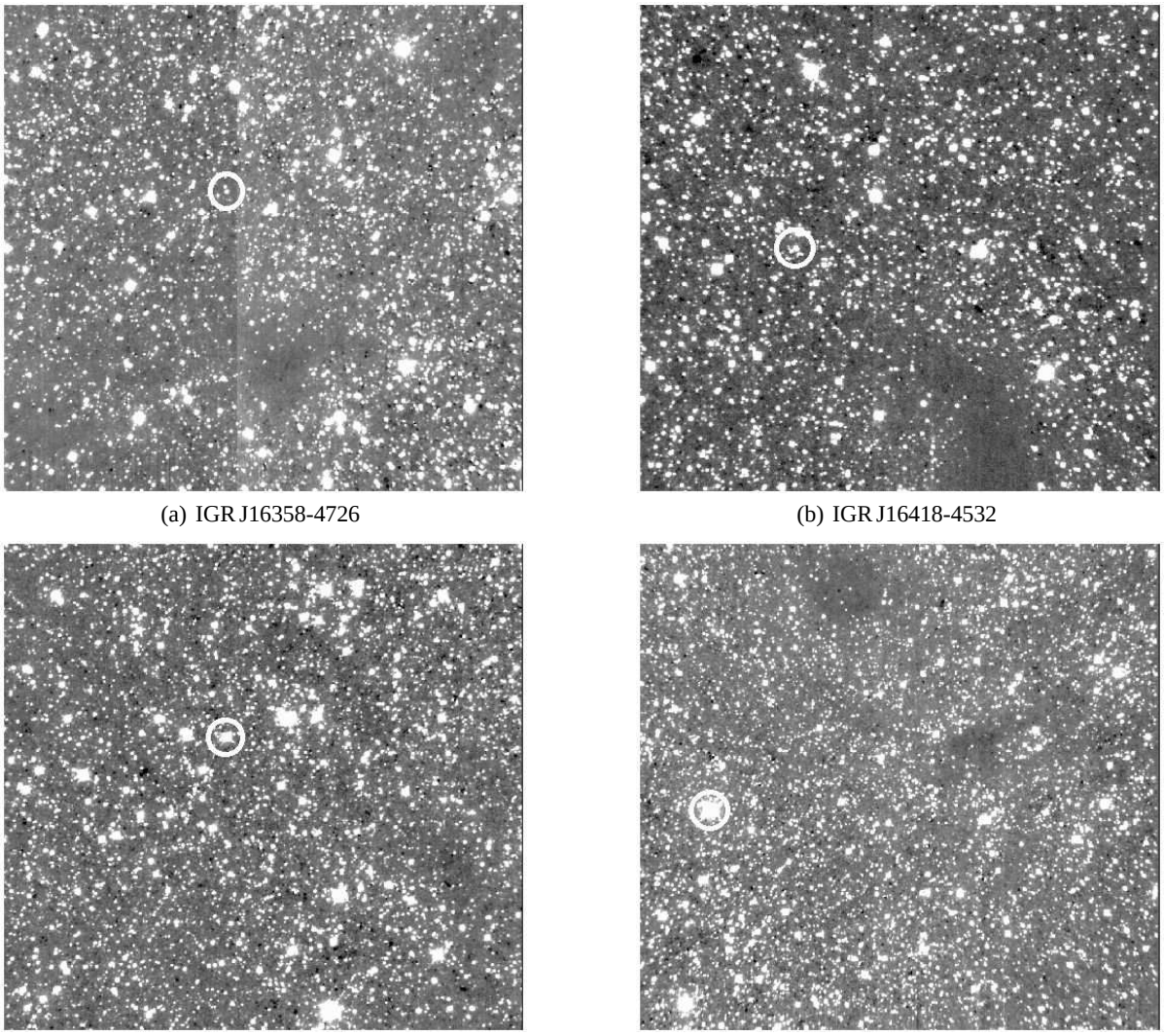

(a) IGR J16358-4726 (b) IGR J16418-4532

(c) IGR J16479-4514 (d) IGR J17391-3021

Fig. 6. Large fields of 4 studied sources exhibiting high absorption along their line of sight. Size: $5.5' \times 5.5'$; North is to the top and East to the left. We overplot a white circle to indicate the position of the *INTEGRAL* sources.

Astronomer's Telegram, 149, 1
Landolt, A. U. 1992, AJ, 104, 340
Lebrun, F., Leray, J. P., Lavocat, P., et al. 2003, A&A, 411, L141
Levine, A. M. & Corbet, R. 2006, The Astronomer's Telegram, 940, 1
Liu, Q. Z., van Paradijs, J., & van den Heuvel, E. P. J. 2000, Astron. Astrophys. Suppl. Ser., 147, 25
Liu, Q. Z., van Paradijs, J., & van den Heuvel, E. P. J. 2006, A&A, 455, 1165
Lutovinov, A., Revnivtsev, M., Gilfanov, M., et al. 2005a, A&A, 444, 821
Lutovinov, A., Rodriguez, J., Revnivtsev, M., & Shtykovskiy, P. 2005b, A&A, 433, L41
Lutovinov, A., Walter, R., Belanger, G., et al. 2003, The Astronomer's Telegram, 155, 1
Malizia, A., Bassani, L., di Cocco, G., et al. 2004, The Astronomer's Telegram, 227, 1
Malizia, A., Bassani, L., Stephen, J. B., et al. 2003, ApJ, 589, L17
Malizia, A., Landi, R., Bassani, L., et al. 2007, ApJ, 668, 81
Markwardt, C. B. & Swank, J. H. 2003, The Astronomer's Telegram, 156, 1
Masetti, N., Morelli, L., Palazzi, E., et al. 2006, A&A, 459, 21
Mill, J. D. 1994, in Proc. SPIE Vol. 2232, p. 200-216, Signal Processing, Sensor Fusion, and Target Recognition III, Ivan Kadar; Vibeke Libby; Eds., ed. I. Kadar & V. Libby, 200–216
Molkov, S., Mowlavi, N., Goldwurm, A., et al. 2003, The Astronomer's Telegram, 176, 1
Munari, U. & Tomasella, L. 1999, A&AS, 137, 521
Munari, U. & Zwitter, T. 1997, A&A, 318, 269
Negueruela, I. 2004, in Revista Mexicana de Astronomia y Astrofisica Conference Series, ed. G. Tovmassian & E. Sion, 55–56
Negueruela, I. & Schurch, M. P. E. 2007, A&A, 461, 631
Negueruela, I., Smith, D. M., Harrison, T. E., & Torrejón, J. M. 2006a, ApJ, 638, 982

Negueruela, I., Smith, D. M., Reig, P., Chaty, S., & Torrejón, J. M. 2006b, in ESA Special Publication, Vol. 604, ESA Special Publication, ed. A. Wilson, 165–170
Nespoli, E., Fabregat, J., & Mennickent, R. 2007, The Astronomer's Telegram, 982, 1
Patel, S. K., Zurita, J., Del Santo, M., et al. 2007, ApJ, 657, 994
Pellizza, L. J., Chaty, S., & Negueruela, I. 2006, A&A, 455, 653
Persson, S. E., Murphy, D. C., Krzeminski, W., Roth, M., & Rieke, M. J. 1998, AJ, 116, 2475
Prat, L., Rodriguez, J., & Hannikainen, D. C. 2008, ArXiv e-prints, 801
Predehl, P. & Schmitt, J. 1995, A&A, 293, 889
Rahoui, F., Chaty, S., Lagage, P.-O., & Pantin, E. 2008, A&A, in press
Revnivtsev, M., Gilfanov, M., Churazov, E., & Sunyaev, R. 2003a, The Astronomer's Telegram, 150, 1
Revnivtsev, M., Tuerler, M., Del Santo, M., et al. 2003b, IAU Circ., 8097, 2
Revnivtsev, M. G., Sunyaev, R. A., Varshalovich, D. A., et al. 2004, Astronomy Letters, 30, 382
Rodriguez, J., Bodaghee, A., Kaaret, P., et al. 2006, MNRAS, 366, 274
Rodriguez, J., Cabanac, C., Hannikainen, D. C., et al. 2005, A&A, 432, 235
Rodriguez, J., Tomsick, J. A., Foschini, L., et al. 2003, A&A, 407, L41
Rupen, M. P., Mioduszewski, A. J., & Dhawan, V. 2003, The Astronomer's Telegram, 152, 1
Russeil, D. 2003, A&A, 397, 133
Sguera, V., Barlow, E. J., Bird, A. J., et al. 2005, A&A, 444, 221
Sguera, V., Bazzano, A., Bird, A. J., et al. 2006, ApJ, 646, 452
Sguera, V., Hill, A. B., Bird, A. J., et al. 2007, A&A, 467, 249
Smith, D. M. 2004, The Astronomer's Telegram, 338, 1
Smith, D. M., Heindl, W. A., Markwardt, C. B., et al. 2006, ApJ, 638, 974
Stephen, J. B., Bassani, L., Molina, M., et al. 2005, A&A, 432, L49
Sunyaev, R., Lutovinov, A., Molkov, S., & Deluit, S. 2003, The Astronomer's Telegram, 181, 1
Swank, J. H. & Markwardt, C. B. 2003, The Astronomer's Telegram, 128, 1
Tauris, T. M. & van den Heuvel, E. P. J. 2006, Formation and evolution of compact stellar X-ray sources (Compact stellar X-ray sources), 623–665
Thompson, T. W. J., Tomsick, J. A., Rothschild, R. E., in't Zand, J. J. M., & Walter, R. 2006, ApJ, 649, 373
Thompson, T. W. J., Tomsick, J. A., Zand, J. J. M. i., Rothschild, R. E., & Walter, R. 2007, ApJ, 661, 447
Tomsick, J. A., Chaty, S., Rodriguez, J., et al. 2006, ApJ, 647, 1309
Tomsick, J. A., Lingenfelter, R., Corbel, S., Goldwurm, A., & Kaaret, P. 2004a, in ESA SP-552: 5th INTEGRAL Workshop on the INTEGRAL Universe, ed. V. Schoenfelder, G. Lichti, & C. Winkler, 413–416
Tomsick, J. A., Lingenfelter, R., Corbel, S., Goldwurm, A., & Kaaret, P. 2004b, The Astronomer's Telegram, 224, 1
Tomsick, J. A., Lingenfelter, R., Walter, R., et al. 2003, IAU Circ., 8076, 1
Türler, M., Balman, S., Bazzano, A., et al. 2007, The Astronomer's Telegram, 1019, 1
Walter, R., Bodaghee, A., Barlow, E. J., et al. 2004a, The Astronomer's Telegram, 229, 1
Walter, R., Courvoisier, T. J.-L., Foschini, L., et al. 2004b, in ESA Special Publication, Vol. 552, 5th INTEGRAL Workshop on the INTEGRAL Universe, ed. V. Schoenfelder, G. Lichti, & C. Winkler, 417–422
Walter, R., Zurita Heras, J., Bassani, L., et al. 2006, A&A, 453, 133
Zurita Heras, J. A., de Cesare, G., Walter, R., et al. 2006, A&A, 448, 261

Table 8: Spectroscopy results. We indicate the name of the sources, the identification of the lines, the rest wavelength (μm), the fitted central wavelength (μm), the flux (in erg $s^{-1}cm^{-2}$ for optical spectra and in arbitrary units for NIR spectra), the equivalent width (EQW in Å), and Full Width Half Maximum (FWHM in Å). T stands for telluric.

Source	Identification	λ	λ_{fit}	Flux	EQW	FWHM
IGR J16320-4751						
	Pa(7-3)	1.005	1.0052	1296.88	-3.773±1.3	55.6
			1.1757	855.62	-1.889	51.35
			1.2609	673.3	-1.275	29.4
			1.5064	689.659	-0.9421	8.044
	Br(17-4)	1.544	1.5442	1214.05	-1.529±0.4	12.76
			1.5479	2708.57	-3.044	112.4
			1.5829	0.0120243	-0.175554	14.6
			2.0998	2160.39	-1.656	88.75
	Br(7-4)/HeI	2.166/2.166	2.1661	7327.22	-5.454±1.0	114.6
	T		2.2962	-10695.5	7.402	51.66
	T		2.3248	-8645.31	6.087	38.76
IGR J16358-4726						
	HeII	1.0133	1.0138	-331.65	24.01	7.408
			1.1935	803.177	-9.219	2.876
	HeII	1.2914	1.2908	878.037	-5.591	25.71
	HeI	1.2971	1.2966	-285.973	1.77	12.26
	?		1.5061	5060.16	-14.96	25.61
	?		1.5839	3229.4	-7.776	25.37
			1.6135	2407.31	-5.477	21.55
			1.6701	-1731.86	10.56	46.58
	Br(11-4)	1.681	1.6811	5716.71	-40.69	133.3
	Br(10-4)	1.737	1.7177	1292.73	-7.716	46.55
			1.7662	-2008.36	10.33	40.9
			1.7906	902.755	-4.666	13.32
			1.8000	-1825.61	9.3	23.42
	Br(9-4)	1.818	1.8206	3066.46	-15.68	92.93
	Br(8-4)	1.945	1.9448	561.476	-2.306	14.81
	FeII?	1.9746	1.9811	1281.53	-5.106	2.16
			2.0018	-4330.84	16.86	38.31
	HeI?	2.058	2.0566	-2011.82	7.386	30.4
			2.1216	944.583	-3.257	23.41
			2.1518	-2205.66	7.095	47.87
	Br(7-4)	2.166	2.1643	1585.54	-5.174	70.49
	[FeII]	2.224	2.2223	3877.44	-12.85	126.6
	HeI	2.3069	2.2934	-1053.51	3.128	17.71
IGR J16479-4514						
			0.9811	417.44	-39.77	28.98
			1.0597	282.616	-8.639	5.383
			1.1293	661.497	-10.13	69.46
			1.2616	376.308	-2.184	5.55
	HeII?	1.3150	1.3178	-489.818	2.034	17.33
			1.4602	336.183	-0.7073	7.066
			1.4679	-280.531	0.5932	7.727
	HeII	1.4882	1.4876	595.672	-1.141	15.05
	Br(23-4)	1.504	1.5046	2512.46	-4.622	39.73
	Br(19-4)	1.526	1.5269	-1037.44	1.767	18.67
	FeII	1.576	1.5760	1858.42	-2.719	35.1
	Br(14-4)	1.588	1.5900	3130.59	-4.995	70.96
	HeI	1.70	1.6998	-1075.65	1.29	22.05

Table 8: continued.

Source	Identification	λ	λ_{fit}	Flux	EQW	FWHM
			1.7891	-2371.63	2.32	20.62
	Br(8-4)	1.945	1.9475	8758.25	-6.548	92.96
			1.9822	4953.06	-3.442	38.83
			2.0076	-22693.7	15.46	192.7
			2.0547	-4648.77	2.992	90.7
	HeI	2.1126	2.1117	-2376.81	1.379	30.27
	Br(7-4)/HeII	2.166/2.166	2.1658	6605.93	-3.652	51.56
			2.2818	2197.39	-1.054	47.44
	T		2.3294	-2606.04	1.184	22.37
IGR J17252-3616						
	HeI		0.7268	9.590E-17	-61.37	32.97
			0.7375	6.308E-17	-34.66	21.14
			0.7622	-1.29E-16	48.04	66.65
			0.7719	1.136E-16	-39.71	37.44
			0.7788	-1.06E-16	22.64	31.12
	T		0.8277	-1.30E-16	31.32	26.38
			0.8341	9.047E-16	-195.9	39.92
	Pa18	0.8437	0.8440	6.046E-16	-106.5	44.48
			0.8819	1.176E-15	-169.9	58.22
			0.8921	6.742E-16	-91.68	46.02
			0.9301	5.538E-16	-50.68	33.24
			0.9397	1.435E-16	-15.17	21.22
			0.9783	5.476E-16	-48.98	57.03
			1.1933	17258.4	-1.55	6.047
	HeII	1.2719	1.2717	-205225.	12.25	116.1
			1.3652	-1927788.	80.62	151.6
	FeII?	1.576	1.5774	170625.	-4.023	63.2
	Br(13-4)	1.611	1.6200	167968.	-3.916	95.54
	PCyg-		2.0555	-277866.	5.281	63.73
	HeI PCyg+	2.0587	2.0597	163020.	-3.08	23.96
	HeI	2.1126	2.1129	-105139.	2.004	29.24
	HeII	2.1891	2.1894	158546.	-3.309	63.66
			2.3190	-203026.	3.913	25.96
IGR J17391-3021						
	NaD	0.5780	0.5786	-9.84E-15	2.512	29.57
	NaD	0.5890	0.5894	-5.74E-15	1.316	16.76
			0.6141	7.903E-15	-1.462	28.81
			0.6183	-9.74E-15	1.736	31.93
	HeII		0.6286	-1.18E-14	2.01	15.24
	Hα	0.6562	0.6568	2.207E-14	-2.804	23.84
	T		0.6888	-7.97E-14	7.934	52.38
			0.7068	-7.77E-15	0.6783	16.38
	T		0.7189	-2.15E-14	1.767	24.4
			0.7395	9.707E-15	-0.7171	32.32
			0.7458	3.928E-15	-0.2813	11.34
	T		0.7629	-6.50E-13	41.87	78.06
			0.7931	-1.15E-14	0.6468	22.8
			0.8171	-5.01E-14	2.624	41.
			0.8237	-2.64E-14	1.349	18.94
	T		0.8290	-4.75E-15	0.241	22.14
	Pa20	0.8392	0.8388	-1.62E-15	0.07962	8.758
	Pa16	0.8502	0.8505	-1.11E-14	0.5035	13.02
	Pa15	0.8545	0.8552	-1.23E-14	0.5532	18.17
	NI	0.8703	0.8712	1.028E-13	-4.347	50.04
	Pa12	0.8750	0.8756	-3.44E-14	1.348	22.97

Table 8: continued.

Source	Identification	λ	λ_{fit}	Flux	EQW	FWHM
			0.8868	-4.96E-14	1.887	25.83
			0.9006	-1.66E-13	6.293	49.69
			0.9118	7.353E-15	-0.2933	17.46
			0.9201	4.781E-14	-1.887	28.79
			0.9230	-4.13E-14	1.545	22.38
			0.9349	-5.66E-13	22.48	64.58
			0.9423	-1.49E-12	57.2	309.8
			0.9447	-2.00E-12	72.96	274.8
			0.9504	-8.41E-13	32.56	178.7
	Pa(8-3)	0.954	0.9550	-1.19E-13	4.949	44.28
			0.9712	1.268E-13	-4.463	36.45
			0.9768	-2.08E-13	6.634	73.77
			0.9930	7.416E-13	-25.57	218.4
			1.0111	1.372E-14	-0.4479	13.33
			1.0093	5.657E-14	-1.853	34.91
	Pa(7-3)/HeII	1.005/1.0049	1.0053	-6.23E-14	1.959	25.14
	HeII	1.0133	1.0133	-1.24E-14	0.4036	12.24
			0.9710	13487.8	-2.658	24.21
	Pa(7-3)/HeII	1.005/1.0049	1.0047	-3997.88	0.7305	9.054
			1.0123	-4141.89	0.7398	9.734
	HeI-D	1.0832-3	1.0834	45732.6	-7.06	42.2
	Pa(6-3)/HeII	1.094/1.0938	1.0937	-9981.06	1.472	15.88
	HeI	1.1972	1.1971	-11849.5	1.522	15.93
			1.2275	8130.68	-1.014	27.2
			1.2609	-7058.26	0.851	1.225
	HeI	1.2789	1.2787	-7781.74	0.9251	9.955
	Pa(5-3)/HeII	1.282/1.2817	1.2812	24041.7	-2.847	69.16
	OI	1.3165	1.3178	-9810.79	1.124	10.69
	Br(23-4)	1.504	1.5034	33968.9	-3.427	39.53
	Br(19-4) PCyg-	1.526	1.5269	-10867.7	1.074	11.76
	PCyg+		1.5296	2753.08	-0.2737	7.687
	Br(17-4)	1.544	1.5449	-5302.73	0.5161	12.05
	Br(15-4)/HeII PCyg-	1.571/1.5719	1.5720	-8690.81	0.816	11.44
	PCyg+		1.5763	28064.4	-2.625	34.17
	HeII?	1.6241	1.6286	-14464.6	2.554	83.49
	HeII	1.6584	1.6591	-8012.45	1.407	59.07
	HeI PCyg-	1.7007	1.7001	-9883.17	1.721	25.47
	PCyg+		1.7108	7183.83	-1.248	46.05
	Br(10-4)/HeII	1.737/1.7355	1.7345	18147.7	-3.105	82.78
	?		2.0023	48773.3	-8.054	53.72
	?		2.0227	-8537.24	1.394	54.94
	HeI	2.0587	2.0583	-19765.2	3.163	32.95
	NIII+CIII	2.116	2.1157	11898.8	-1.87	28.88
	Br(7-4)/HeI	2.166/2.166	2.1652	14485.3	-2.267	48.56
	HeII	2.1891	2.1887	-5196.59	0.8194	24.93
IGR J18027-2016						
	Hζ	0.3889	0.3872	-1.64E-16	85.36	13.75
	Hδ	0.4101	0.4109	1.403E-15	INDEF	13.79
	HeII	0.4200	0.4201	-7.06E-16	2460.	8.549
			0.4614	-5.94E-16	79.65	7.906
	HeII	0.4686	0.4696	2.762E-16	-28.62	20.08
	Hβ?	0.4861	0.4901	9.769E-16	-75.71	10.23
			0.5180	-7.98E-16	51.37	9.967
			0.5460	2.099E-16	-7.693	12.53
	NaD	0.5890	0.5884	-1.99E-16	3.885	20.76

Table 8: continued.

Source	Identification	λ	λ_{fit}	Flux	EQW	FWHM
			0.6251	3.172E-16	-5.072	42.17
	Hα	0.6562	0.6570	6.033E-16	-6.788	44.4
	T		0.6885	-1.21E-15	10.03	59.22
			0.7111	-6.80E-17	0.4671	7.604
			0.7187	-1.65E-16	1.096	21.06
			0.7380	3.866E-16	-2.221	43.12
			0.7415	-3.43E-16	1.845	31.
			0.7621	-8.49E-15	40.47	66.51
			0.8077	3.062E-16	-1.061	20.52
	T		0.8240	-4.18E-16	1.409	10.03
			0.8345	1.376E-15	-4.163	33.41
			0.8493	-1.38E-15	3.771	22.71
			0.8819	2.979E-15	-7.014	50.99
			0.8914	2.231E-15	-5.194	42.9
			0.9001	-1.79E-15	4.164	40.1
			0.9348	-5.29E-15	13.54	50.03
			0.9441	-1.93E-15	5.08	34.31
	Pa(8-3)	0.9549	0.9551	-4.02E-15	9.739	83.46
			1.0193	169299.	-16.81	67.81
	HeI	1.1016	1.1026	-188368.	13.04	111.4
			1.2747	-267133.	11.87	89.39
	Br(17-4)?	1.544	1.5484	257952.	-8.298	116.5
			1.5813	-137910.	4.266	59.41
	PCyg-		1.6010	-87404.2	2.733	35.72
	PCyg+?		1.6060	46540.9	-1.455	7.072
	HeII?	1.6241	1.6220	-105641.	3.331	41.99
	Br(12-4)? PCyg-	1.641	1.6439	-340789.	10.27	82.88
	PCyg+		1.6493	-14621.9	0.4325	1.403
	PCyg-		2.0033	-644298.	25.66	59.55
	PCyg+		2.0103	123941.	-4.991	29.17
			2.2983	-299051.	14.65	55.77
	T		2.3262	-103670.	5.96	25.2
	T		2.3563	-226137.	14.08	59.82
	T		2.3867	-113159.	7.989	29.05
	T		2.4189	-141757.	9.892	37.36
IGR J19140+0951						
			0.9787	254.752	-0.5518	8.255
	Pa(7-3)	1.005	1.0053	-179.359	0.397	10.52
	-		1.0081	113.557	-0.2515	8.25
	-		1.0595	193.383	-0.4397	6.494
	-		1.1919	554.	-1.31	15.17
	-		1.2613	247.094	-0.5914	7.01
	Pa(5-3)/HeII	1.282/1.2817	1.2821	-359.765	0.86	13.84
	-		1.5830	1002.7	-3.077	83.78
	-		1.5845	-414.155	0.9797	7.817
	Br(14-4)?	1.588	1.5895	-517.017	1.205	29.69
	HeII	1.6584	1.6592	324.516	-0.9892	12.57
			1.6687	1036.81	-3.168	95.57
			1.6834	-149.388	0.4517	7.682
	HeII	1.8725	1.8728	1335.31	-4.457	11.47
			2.0070	-12037.2	37.72	187.7
	HeI	2.0587	2.0600	563.242	-1.878	30.69
	HeI	2.1126	2.1129	169.253	-0.5294	18.93